INFORMATION TO USERS

This manuscript has been reproduced from the microfilm master. UMI films the text directly from the original or copy submitted. Thus, some thesis and dissertation copies are in typewriter face, while others may be from any type of computer printer.

The quality of this reproduction is dependent upon the quality of the copy submitted. Broken or indistinct print, colored or poor quality illustrations and photographs, print bleedthrough, substandard margins, and improper alignment can adversely affect reproduction.

In the unlikely event that the author did not send UMI a complete manuscript and there are missing pages, these will be noted. Also, if unauthorized copyright material had to be removed, a note will indicate the deletion.

Oversize materials (e.g., maps, drawings, charts) are reproduced by sectioning the original, beginning at the upper left-hand corner and continuing from left to right in equal sections with small overlaps.

ProQuest Information and Learning
300 North Zeeb Road, Ann Arbor, MI 48106-1346 USA
800-521-0600

SC

Radiative proton capture study of ^{59}Cu

by

Raymond Gauthier

Submitted in partial fulfillment
of the requirements for the degree
of Master of Science.

Department of Physics
Faculty of Science and Engineering
University of Ottawa
Ottawa, Canada

March, 1970

Approved for the

Department of Physics

Date July 10, 1970.

Chairman

Hommage de profonde gratitude

à mes parents.

ABSTRACT

Enriched ^{58}Ni targets were bombarded with H_1^+ ions of energy varying from 900 to 2000 kev. A 30 cc Ge(Li) detector was used to detect the gamma rays following the radiative proton capture. Nine resonances were studied and the spectra analysed to give gamma ray branching ratios and energy levels in ^{59}Cu. From the decay of the resonance level for E_p = (1423.64 ± .43) kev and E_p = (1843.45 ± .56) kev the Q of the reaction was calculated to be (3418.5 ± 2.4) kev. Partial proton and gamma ray widths were determined by integration of the 1303 kev and 878 kev gamma ray peaks following the β^+ disintegration of ^{59}Cu. A Doppler shift measurement performed on the E_p = 1424 kev resonance level gave a value $\tau < 2 \times 10^{-15}$ second.

ACKNOWLEDGMENT

I am indebted to Dr. B.A. Logan and Dr. H.L. Pai, of this university, for their help, their interest and most useful discussions.

I would like to express special thanks to Dr. I.L. Fairweather, supervisor, for his help and interest in the work, for his useful suggestions about the presentation of this thesis and for some financial support.

Thanks to Dr. A.L. Carter for making available not only the stabilized spectrometer system, without which a part of the work presented in this thesis could not have been done, but also the pulse height analysis program which was used in the data analysis.

I would like also to thank all those persons involved with the operation and maintenance of the Dymamitron accelerator for their patience and co-operation.

Finally thank you to Mrs. Roger Gauthier for typing this thesis.

The financial support of the Province of Ontario is greatefully acknowledged.

TABLE OF CONTENTS

LIST OF FIGURES

LIST OF TABLES

1. INTRODUCTION

With yields in the region of 10^{-10} gamma rays per proton, radiative proton capture reactions on light elements ($A < 20$) using NaI detectors has proven to be a very useful and productive tool in nuclear spectroscopy. The extension of radiative proton capture work to elements of higher Z using the new high resolution but low efficiency Ge(Li) gamma ray detector requires a high current proton beam. The beam current that one can expect to extract from a Dynamitron makes this machine most suitable for continuing the radiative proton capture work to heavier elements using the latest detectors.

The odd-mass Cu isotopes have been the object of several theoritical studies during recent years. Inelastic scattering of α particles on Ni isotopes (Cr.,60) and Coulomb excitation experiments (Te.,He., 56) on ^{63,65}Cu suggest some type of collective vibrational motion for the lowest levels of the odd-Cu isotopes. Quite good agreement was obtained with experiments by calculations based on some type of

core excitation model (Bo.,Va.,62) in which the low levels of the odd-Cu isotopes are described in terms of the coupling of the odd proton outside the Z = 28 closed shell to one or more excited states of the nickel core. However recent stripping experiments (Bl.,64) have shown that the excited states of the odd-Cu isotopes have large single particle strengths. The large single particle strengths suggest a shell model approach (Bo.,Bo.,68). In view of the theoretical interest of these isotopes additional information is being sought throught radiative proton capture reactions using the joint Carleton - Ottawa University Dynamitron accelerator. Some data as been obtained at several resonances and analysed to give gamma ray branching ratios and partial proton and gamma ray widths for ^{59}Cu.

2. TARGETS: PREPARATION AND PROTECTION

The target backing consists of a 2 1/4 inch diameter copper disc 1/8 inch thick. For low background conditions 1/1000 of an inch of gold is electroplated on the disc. This thickness is sufficient to stop all protons up to 2 Mev in energy. ^{58}Ni is electroplated on to the central part of the disc which is one inch in diameter. The procedures for the preparation of the NiO solution and the plating are described in reference (Bu.,Go.,57). The enriched nickel oxide compound was obtained from the Atomic Energy Research Establishment, Harwell England. The isotopic abundance of ^{58}Ni is stated to be 99.76% with 0.11% and 0.12% of ^{60}Ni and ^{62}Ni respectively. The target and target chamber assembly is shown in figure 2:1. Direct water cooling is used to prevent the target from over heating and thus to avoid deterioration. Ion pumps were used instead of diffusion pumps on the beam line in order to eliminate target contamination due to oil vapours. A cylindrical cold finger was used before the target chamber to condense

figure 2.1

TARGET CHAMBER

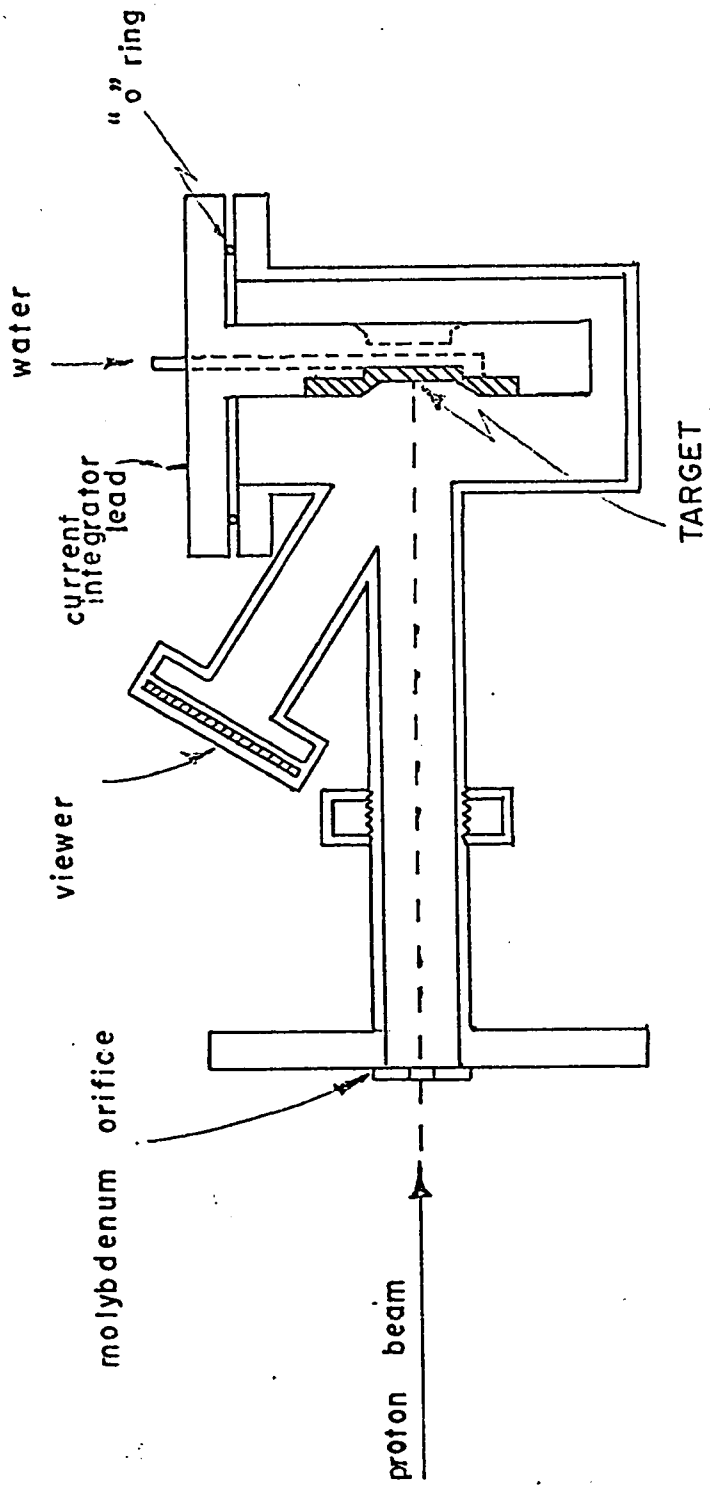

contaminating vapours thereby reducing condensation on the target.

3. RESONANT GAMMA RAY YIELD

Excitation curves were obtained using a 3" x 3" NaI (Tl) detector which was placed at approximately 90^{o} with respect to the direction of the proton beam and at a distance of about twelve inches from the target. Figure 3.1a shows the relative thick target yield of gamma rays having an energy greater than 1.7 Mev. The target used to obtain this excitation curve was measured to be approximately 20 kev thick for 1 Mev protons. The proton energy was increased by steps of 5 kev and for each step a charge of 1.3 milli-coulombs was collected. The beam current was 10 micro-amperes. Figure 3.1a shows only those ^{58}Ni (p,γ) ^{59}Cu resonances which were well above the background level in the 900 kev to 1500 kev proton energy region. The 20 kev target was much thicker than the energy resolution of the accelerator and it was decided to prepare a thinner target in order

$^{58}Ni\ (p,\gamma)^{59}Cu$

figure 3.1a

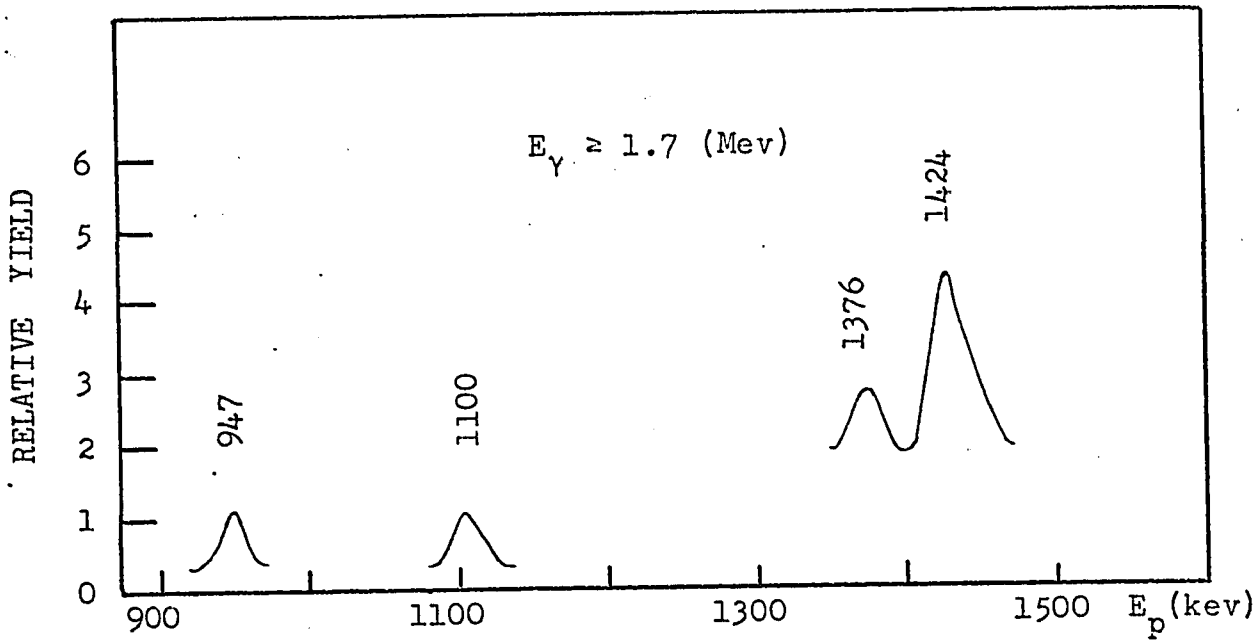

figure 3.1b

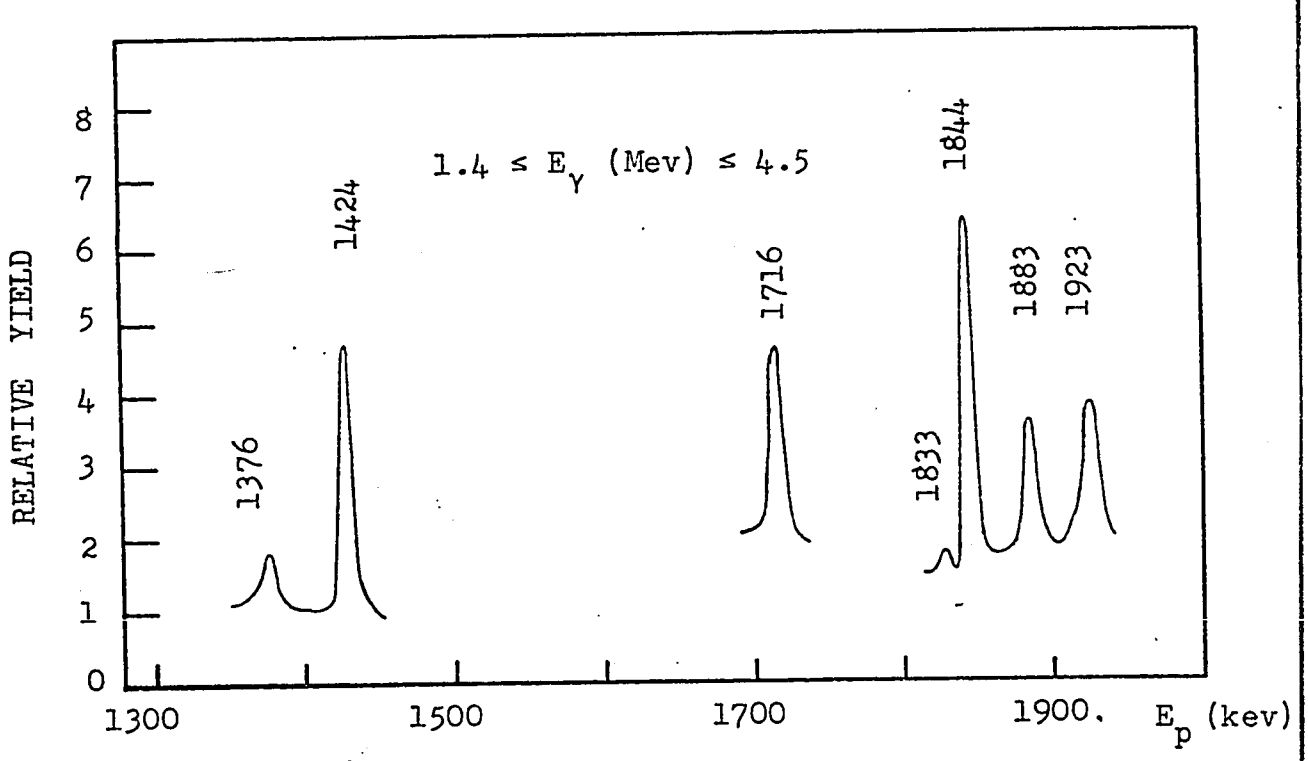

to be able to better separate adjacent resonances. The thickness of this target was determined from a measurement of the width observed for the 1424 kev resonance. Steps of 3 kev were taken and the gamma ray yield obtained for the region 1.4 Mev $\leq E_\gamma \leq$ 3.5 Mev in order to exclude gamma rays from the well known $^{19}F\ (p,\alpha\gamma)\ ^{16}O$ which are very prominent on account of the high cross-section for this reaction.

Using the relation:

$$(T)^2 = (\Delta p)^2 + (t)^2 + (\Gamma)^2 \qquad (1)$$

where T is the observed half-width of the resonance, Δp the beam energy spread which was determined to be about 6 kev at 1 Mev and Γ is the total natural width of the resonance which is of the order of electron volts and can in this case be neglected.

This gives a value for the target thickness of 7 kev. Proceeding similarly as for figure 3.1a a yield curve was obtained using this target for proton energies from 1200 kev to 2000 kev for gamma rays in the region 1.4 Mev $\leq E_\gamma \leq$ 4.5 Mev and with 15 micro-

amperes beam current. The results are shown in figure 3.1b. Identification of background resonances was facilitated by using a table (Bu.,59) of well known radiative capture reaction resonances for many different target isotopes. The principle background arises from proton resonances for $(p,\alpha\gamma)$ reactions on ^{19}F and ^{15}N targets. (See section 8.3).

4. GAMMA RAY SPECTROMETER

4.1 GENERAL DESCRIPTION

The gamma ray spectrometer consists of a Ge(Li) detector and its associated electronics. A block diagram of spectrometer used is shown in figure 4.1. The spectrometer without the Northern Scientific digital spectrum stabilizer will be referred to as system no. 1. For system no. 1 the electronics is located in a air conditioned room. The improved version of the spectrometer we will designate as system no. 2, and this comprises system no. 1 plus the spectrum stabilizer. All the linear stages of the electronics of system no. 2, excluding the preamplifier, was kept in a thermally insulated rack. The preamplifier was thermally insulated

figure 4.1

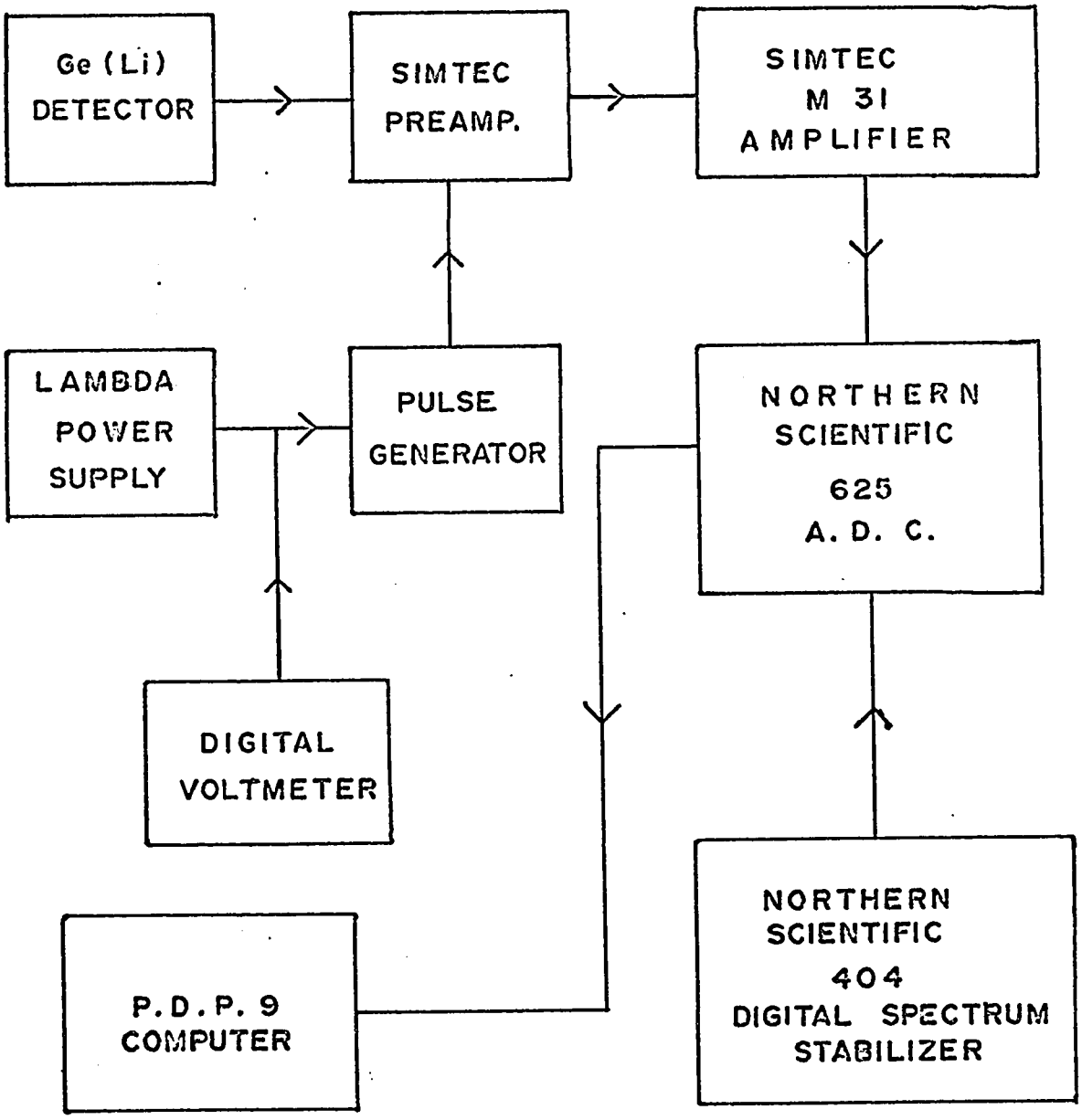

BLOCK DIAGRAM OF GAMMA RAY SPECTROMETER

rack. The preamplifier was thermally insulated by itself.

4.2a DESCRIPTION OF Ge(Li) DETECTOR

The Ge(Li) detector used was obtained from Ortec and is of the open-ended coaxial type with an active volume of 28.3 cm^3. An actual scale drawing is given in figure 4.2a. The optimum energy resolution is 2.6 kev for the ^{60}Co 1333 kev gamma ray. During most of the experimental runs the resolution was typically 12 kev for 6 Mev gamma rays.

4.2b EFFICIENCY CALIBRATION

A set of standardized gamma sources of known intensity was used to determine the absolute efficiency of the full energy peak in the energy range below 3 Mev. The sources were obtained from the International Atomic Energy Agency and calibrated by them to within 1% typically. The absolute efficiency is defined as:

$$\epsilon = \frac{\text{no. of gamma rays detected}}{\text{no. of disintegrations}} \qquad (2)$$

The sources used are listed in table 4.2b. The efficiency was determined by placing the sources on the backing where the beam hit the target and by positioning the detector at an angle of 125° with

TO SCALE DRAWING OF OPEN-ENDED COAXIAL Ge(Li) DETECTOR

figure 4.2a

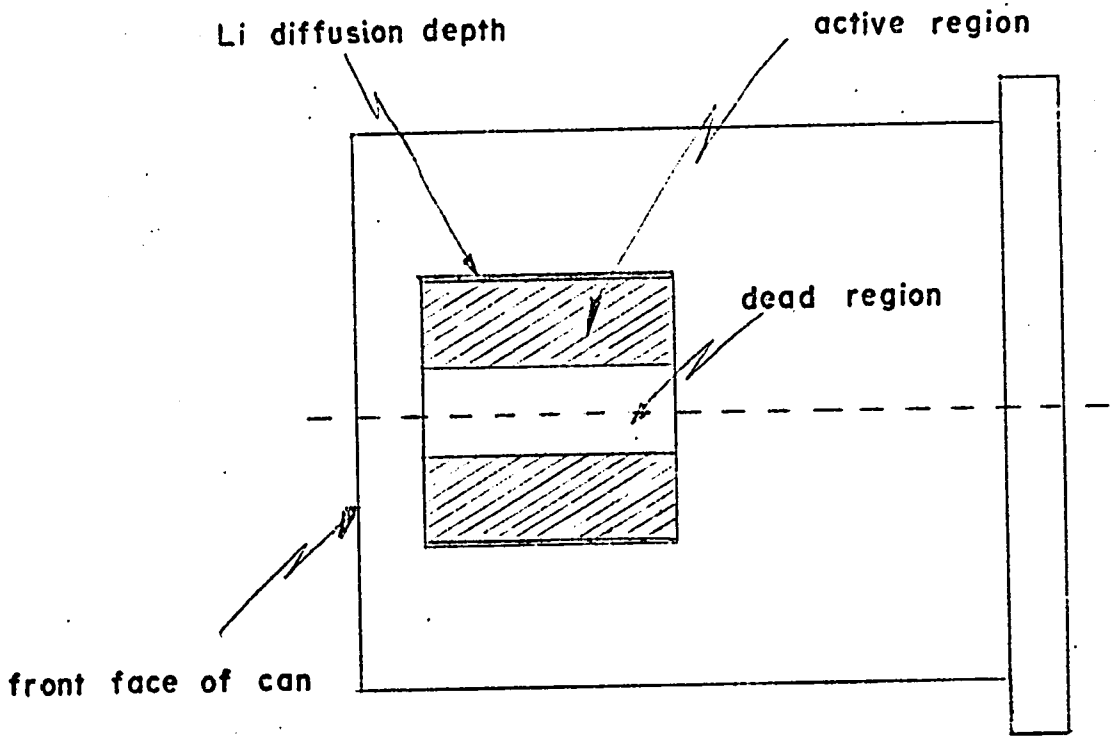

table 4.2b

CALIBRATION SOURCES FOR FULL ENERGY PEAK EFFICIENCY

Element	E_γ(kev)	ϵ
^{57}Co	122	$(7.13\pm0.53)\times10^{-4}$
^{139}Ce	166	$(6.47\pm0.51)\times10^{-4}$
^{203}Hg	279	$(2.86\pm0.23)\times10^{-3}$
^{22}Na	511	$(2.76\pm0.30)\times10^{-3}$
^{137}Cs	667	$(1.08\pm0.02)\times10^{-3}$
^{54}Mn	835	$(9.10\pm0.40)\times10^{-4}$
^{88}Y	898	$(8.00\pm0.50)\times10^{-4}$
^{60}Co	1173	$(6.00\pm0.25)\times10^{-4}$
^{22}Na	1273	$(5.18\pm0.20)\times10^{-4}$
^{60}Co	1333	$(4.81\pm0.10)\times10^{-4}$
^{88}Y	1836	$(3.51\pm0.20)\times10^{-4}$
$*^{24}Na$	2753	$(1.98\pm0.05)\times10^{-4}$

respect to the direction of the proton beam and at a distance of 6 cms from the target. This reproduced the experimental arrangement for the $^{58}Ni\ (p,\gamma)\ ^{59}Cu$ measurements. Several independent determinations of ϵ were made for each gamma ray energy. The standard deviation was calculated for each point and used as the uncertainty in the measurement. Since the calibration was done with "point" sources except for ^{24}Na which was of the same size as the beam spot, i.e. approximately 3/8" in diameter, correction due to the finite size of beam was calculated using the equation (Bur.,49) given below:

$$G = 0.5\ (1 - A - B\gamma - C\gamma^2 - D\gamma^3) \qquad (3)$$

where

$$A = \frac{1}{(1 + \delta)^{1/2}}$$

$$B = \frac{3}{8}\frac{\delta}{8\ (1 + \delta)^{5/2}}$$

$$C = -\frac{5}{6}\frac{\delta}{(1+\delta)^{1/2}} + \frac{35}{64}\frac{\delta^2}{(1+\delta)^{9/2}}$$

$$D = \frac{35}{128}\frac{\delta}{(1+\delta)^{9/2}} - \frac{315}{256}\frac{\delta^2}{(1+\delta)^{1/2}} + \frac{1155}{1024}\frac{\delta^3}{(1+\delta)^{13/2}}$$

G is the percentage solid angle subtended by the sensitive volume of the detector, δ is the square of the ratio of the radius of the detector to the source to detector distance and γ is the square of the ratio of the source radius to the source to detector distance. Calculations showed that the point source estimate were 0.5% too large. Results are listed in table 4.2b. The absolute efficiency for the full energy peak of all gamma rays with energies between 122 and 2753 kev is obtained by drawing a smooth curve through the data points (see figure 4.2b). To obtain the full energy peak efficiency for gamma rays greater than 2.753 Mev, the measured absolute efficiencies for all gamma rays from 662 to 2753 kev were corrected for attenuation due to absorption layers between the target and the detector. A straight line extrapolation through these values on a logarithmic plot of absolute

figure 4.2b

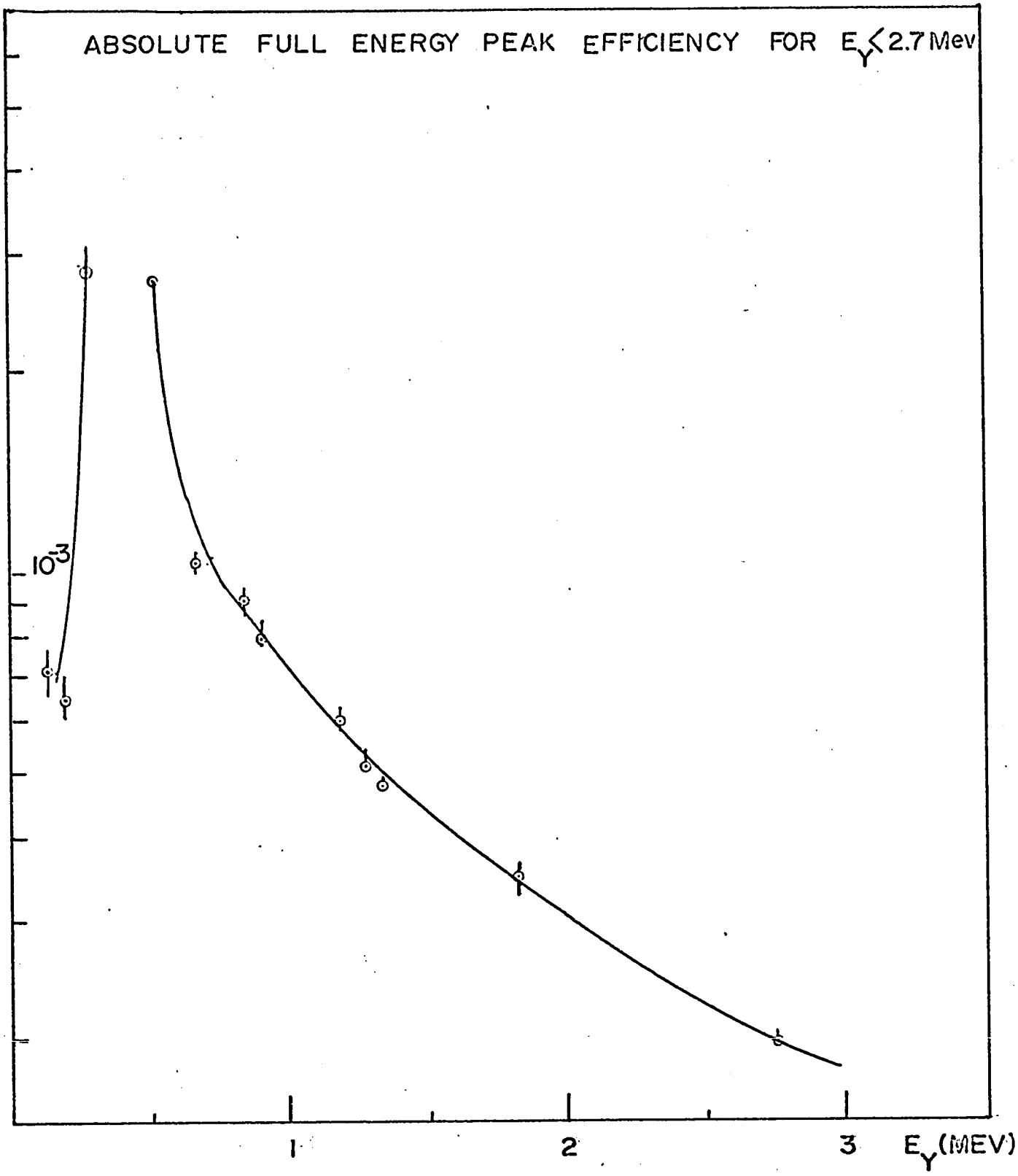
ABSOLUTE FULL ENERGY PEAK EFFICIENCY FOR E_γ < 2.7 Mev
10^{-3}
1
2
3
E_γ (MEV)

efficiency at zero attenuation versus gamma ray energy is expected to be accurate to within 2% (Ka.,67) (Au.,69). Since the attenuation in the region of interest is approximately 6.5% the absolute efficiency curve at this attenuation is shown in figure 4.2c. The absolute efficiency of the escape peaks was determined from the gamma ray spectra obtained during the radiative proton capture study of ^{58}Ni. This was done by taking the ratio of the area under the escape peaks to the area under the corresponding full energy peak. Figure 4.2d shows the curves obtained for the absolute efficiencies of the single and double escape peaks.

* Because of its short lifetime the ^{24}Na source was obtained by neutron irradiation of ^{23}Na. The irradiation was done at A.E.C.L. (Commercial Products Division), Ottawa.

figure 4.2c

ABSOLUTE FULL ENERGY PEAK EFFICIENCY FOR $E_\gamma > 2.7$ MEV

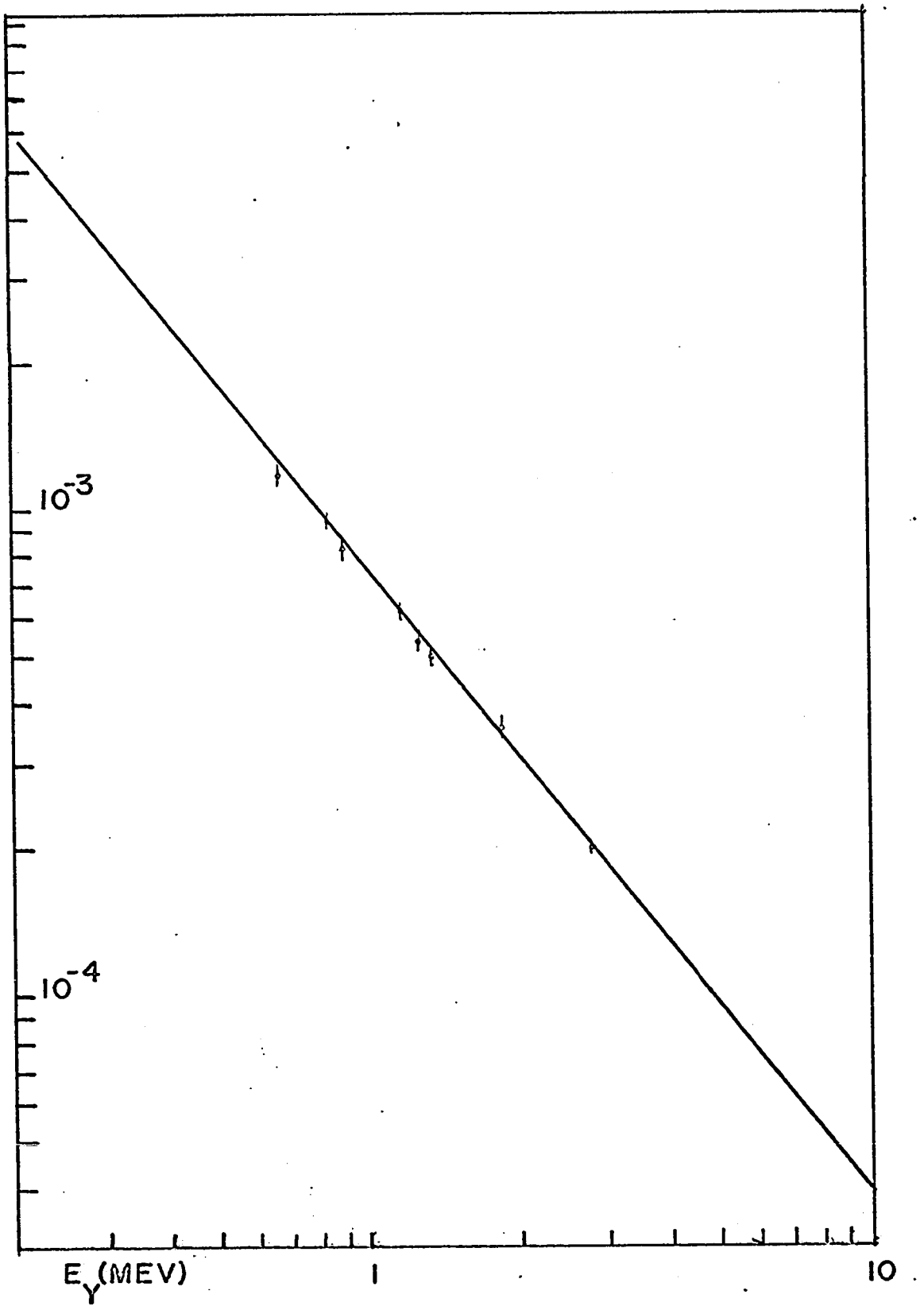

ABSOLUTE EFFICIENCY OF ESCAPE PEAKS figure 4.2d

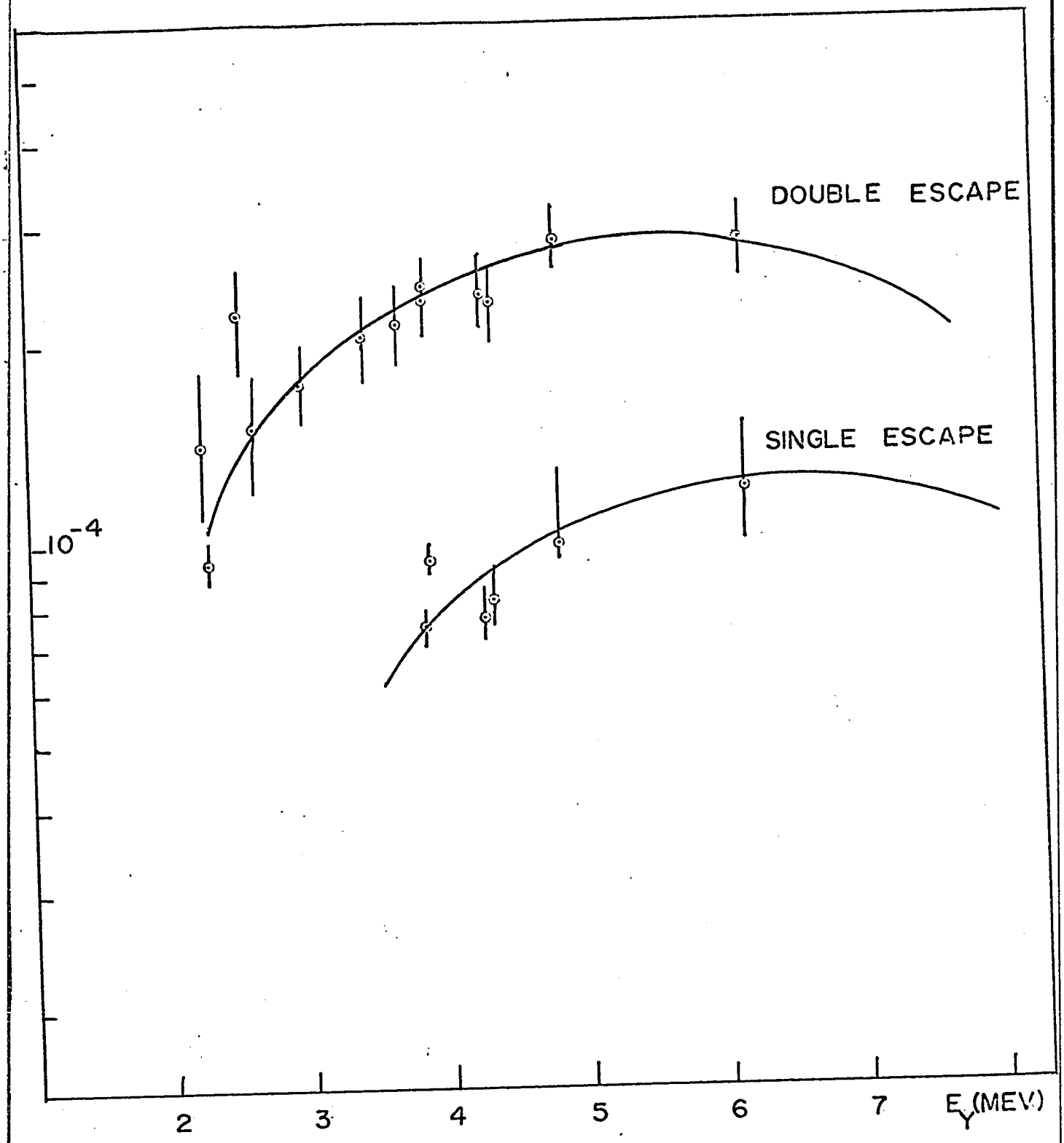

4.3 NON-LINEARITY OF ELECTRONICS: SYSTEM NO. 1

The gamma ray energy calibration can be written as:

$$E = a_0 + a_1 c + a_2 c^2 + \ldots \qquad (4)$$

where E stands for energy and c for the observed channel number. The terms $a_2 c^2 + \ldots$ determine the non-linearity of the electronics. Obviously the energy calibration will vary with changes in the zero level and gain of the electronics. A high precision pulse generator with an applied d.c. voltage known to an accuracy of a few parts per million was used to determine the non-linearity of the electronics. The pulse generator was coupled capacitively to the input stage of the preamplifier with the detector under normal operating conditions. The centroïds of the pulser peaks were determined corresponding to a series of voltage settings and the deviations from the best square linear fit of voltage and centroïd positions were determined. From these the corrections to be applied to the centroïds of the peaks to convert them to the linear fit were determined. The non-

linearity corrections obtained in this way should be the same as those that would be obtained by using gamma rays absorbed in the detector provided the pulse shapes are closely the same. The accuracy in gamma ray energy determination that can be obtained with the above method is limited by temperature fluctuations that can change the gain or zero level during the course of the experiment. The accuracy with which gamma ray energies can be determined after applying the above corrections will be dependent on the precision with which gamma ray peak positions for unknown and calibration lines can be determined from the spectra. An accuracy of ± 4 kev was obtained for spectra having a dispersion of 6 kev/channel and for those having a dispersion of about 2.6 kev/channel the accuracy was ± 3 kev. This precision was checked by comparing the energy value obtained with the best value of the known calibration lines and by calculating energy differences between full energy peaks and their escape peaks.

4.4 NON-LINEARITY OF ELECTRONICS: SYSTEM NO. 2

A more systematic attempt to make precision gamma ray energy measurements possible even over a period of several days was developed by A.L. Carter. In résumé it consists in trying to maintain the temperature of the electronics constant and independent of fluctuations in room temperature and in stabilizing against any residual gain or zero level drifts in the electronic system by means of a spectrum stabilizer. The preamplifier which was located near the target was thermally insulated and the rest of the electronics including the amplifier, the analog to digital converter, the spectrum stabilizer and the pulse generator and associated voltage supply were enclosed in a thermally insulating rack. The pulse generator provides the gain stabilizing pulse when accumulating a spectrum and was also used to generate the sliding pulses for the non-linearity measurements. The exact relationship between voltage and centroïd channel number for the thermally controlled and gain stabilized system was obtained with every precaution taken to eliminate effects due to short term drifts during the measurements. The non-linearity correction curve deduced is shown in

figure 4.4. It is seen that a drift of one channel would only displace the non-linearity curve by one channel and would produce at maximum a change of 0.008 channel in the non-linearity corrections. Because the non-linear terms are little sensitive to drifts, changes in the energy calibration due to changes in the non-linear terms which are caused by drifts makes it a second order effect. The two remaining terms a_0 and $a_1 c$ however are quite sensitive to drifts and can change the energy calibration. A zero level drift would correspond to a change in a_0 and a gain variation would correspond to a change in a_1. The gain variation is magnified by a factor c, so that in order to obtain best gain stabilization possible the amplitude of the stabilizing pulse was such that it occured within the last 50 channels of the fourth quadrant of the A.D.C. (analog to digital converter). The accuracy in determining gamma ray energies with this stabilized system was tested when attempting an angular distribution on the 1424 kev resonance. The test was done in the following way: The centroid of the peak of the 2615 kev gamma ray coming from ThC" was determined after every spectrum accumulated for the 1424 kev

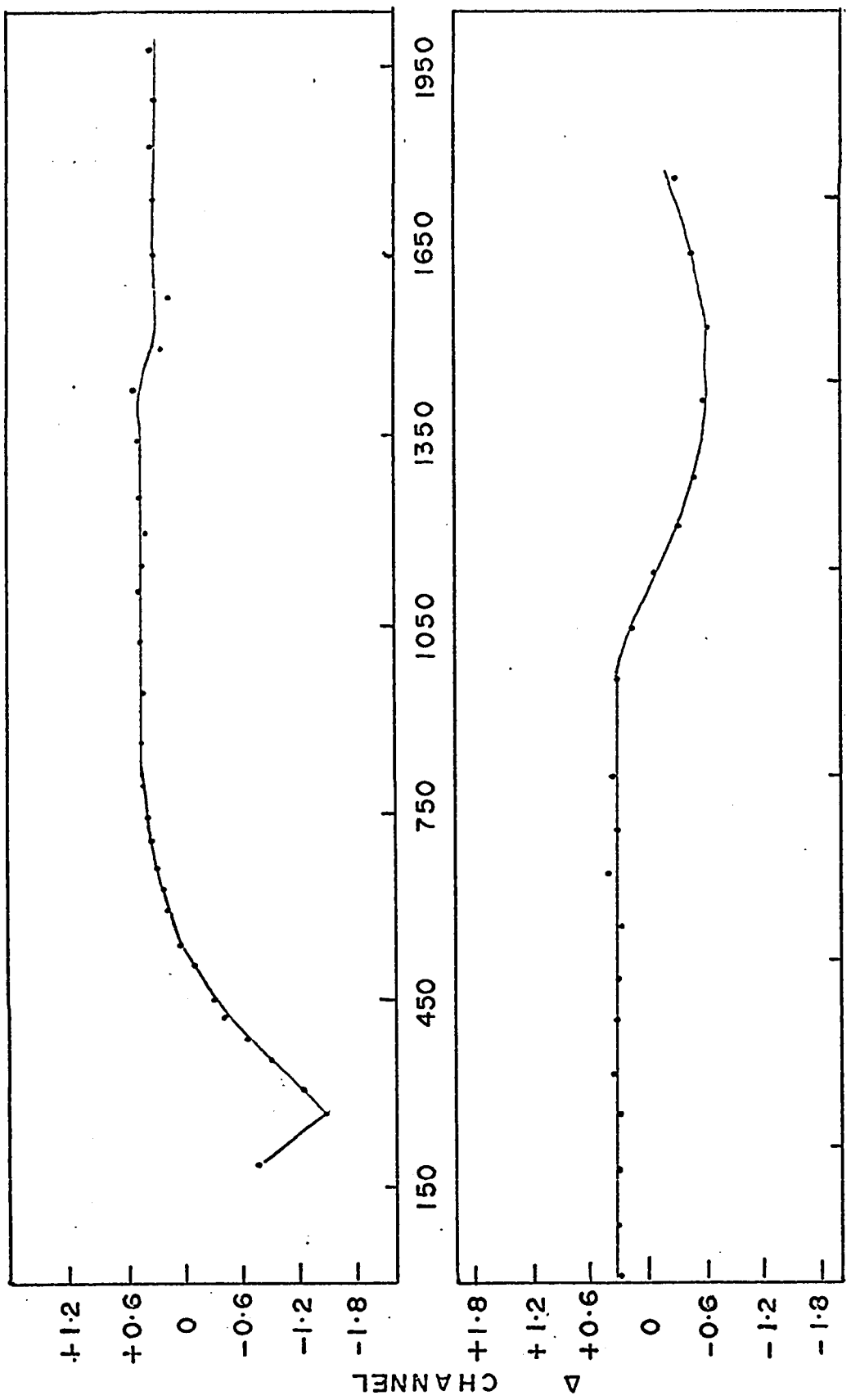
LINEARITY CURVE
Δ CHANNEL
+1·2
+0·6
0
-0·6
-1·2
-1·8
150
450
750
1050
1350
1650
1950
2250
2550
2850
3150
3450
3750
CHANNEL NUMBER

figure 4.4

resonance. Spectra were obtained for four different angles. Once the angular distribution was completed standard gamma ray sources were used to obtain an energy calibration. Then the non-linearity of the electronics was obtained by finding the centroïds of the pulses generated by the sliding pulser. The pulse height ranged from 0.5 to 10 volts and were varied in such a way that a pulse occured at about every 80 channels. The position of several pulser peaks was checked and all repeated within .03 channels. Stability was checked by switching the pulser back to the ten volt reference and remeasuring the corresponding channel number between each point in order to monitor any slight drift. The channel number for each point was then normalized to correspond to the same mean value for the average of the two channel numbers found for the ten volt reference peak measured before and after the measurement of a point. More recently this procedure is simplified by using two standard ultra high precision pulse generators selected alternatively by a mercury relay operating 90^{o} out of phase to both. One is used for gain stabilizing and the second as a precision sliding pulser providing a fast check on the system

non-linearity. A linear least square fit was obtained for the centroïds of the sliding pulser peaks, the deviations from which are shown in figure 4.4 where:

Δ channel = true channel no. - observed channel no.

Then the channel corrections found were used to correct the centroïds of the peaks of the standard gamma ray sources to standard channels of a linear system. A linear least square fit of the corrected peaks of the standard gamma ray sources gave an linear energy calibration such that a_0 = - 126.817 kev, a_1 = 1.8627 kev/channel. Then the five spectra obtained for the 1424 kev resonance were analysed. The centroïd of every peak of the spectra are found and corrected for the non-linearity of the electronics. The corrected centroïd is substituded in the energy calibration equation and the energy of each peak is thus obtained. The background gamma rays occuring in the 1424 kev resonance spectra which have no angular dependence and whose energies are well known are compared in table 4.4 with energies determined from the spectra analysis. The energies of the gamma rays, E_γ, were taken from

table 4.4

SOURCE	E_γ (KEV)	$[E_\gamma - E_\gamma(\text{obs.})]_{max.}$ IN KEV	INTEGRATED COUNTS	$\sigma_{\bar{x}}$ (KEV)
M_0C^2	511.006 ± .002	0.40	40,000	0.01
^{40}K	1460.75 ± .06	0.63	450	0.08
(ThC")	2614.47 ± .10	0.72	120	0.18
$^{19}F(p,\alpha\gamma)^{16}O$	6129.3 ± .4	0.90	400	0.14

(Ma.,68), the statistical uncertainty in the centroid determination $\sigma_{\bar{x}}$ was calculated using the following equation:

$$\sigma_{\bar{x}} = \frac{0.4249 \quad \text{F.W.H.M.}}{(N)^{1/2}} \tag{5}$$

which gives the standard deviation of the mean value for a small sample (Ev.,53). F.W.H.M. stands for the full width of the peak at half maximum height and N stands for the number of measurements in the sample which in this case is the number of counts in the peak. Results are tabulated in table 4.4. $[E_\gamma - E_\gamma \text{ (obs)}]_{max.}$ gives the maximum deviation observed between the calculated and accepted value of the gamma rays over a time of 70 hours. In addition the maximum deviation between corresponding escape peaks and between full energy peaks and their corresponding escape peaks was 1.5 kev and the standard deviation was 0.5 kev. From table 4.4 one sees that the gamma ray energies can easely be determined with a precision of one kev. The statistical uncertainty in the position of the centroid of peaks is much less than the maximum deviation observed even with the best statistics. Results could be improved if the centroid

determination was done after better background subtraction. Background subtraction was achieved by positioning two markers on each side of the peaks, where there may be large background fluctuations, a straight line drawn through these determined the background to be subtracted.

5. EXPERIMENTAL SET UP AND DATA ACCUMULATION

The spectra were taken with the 30 cm^3 Ge(Li) detector. The detector itself was mounted on a turn table rotating about a vertical axis going through the center of the beam spot on the target. The voltage pulses from the detector were encoded by 4096 channel analog to digital converter. The spectrum was stored in the memory of an on line PDP 9 computer. The stored information could be punched out on paper tape, stored on magnetic tape, plotted out and displayed on the screen of an oscilloscope. A pulse height analysis program developed by Dr. A.L. Carter of Carleton University was used to analyse the spectra. With this program centroids, integrated counts and width at half maximum height of peaks could be determined.

6. GAMMA RAY SPECTRA

With spectrometer at stage referred to as system no. 1, for each resonance studied three spectra were taken. Two of these were taken on resonance: one with the detector making an angle of 125° with respect to the direction of the proton beam and for the other it made an angle of 90°. The spectra taken with the detector at the 125° position were used to determine the gamma ray intensities (see section 8.1) while those taken with detector at 90° position gave the unshifted energies of the gamma rays. The third spectrum was taken off resonance at a proton energy such that any possible drift in the proton beam energy could not bring it back on resonance. All peaks occuring in these spectra were taken to be background peaks. An accumulation time of two hours was required on the average to obtain reasonable statistics in a given spectrum with a beam current of 20 microamperes.

Note: These spectra were obtained with system no. 1 because system no. 2 was not available at that time.

7. SPECTRA ANALYSIS

7.1 GAMMA RAY ENERGY DETERMINATION

The energy of each peak is determined from the spectra accumulated at 90^{o}. As mentioned in section 4.3 the centroïds are found and corrected for the non-linearity of the electronics. Background peaks such as ^{40}K peak and the fluorine peaks along with standard gamma ray sources which are used repeatedly during the experiment give the energy calibration.

7.2 TRANSITION INTENSITIES

The gamma ray intensity of each gamma ray appearing in the 125^{o} spectra is determined by dividing the integrated full energy peak by the absolute full energy peak efficiency of the detector. The competing process of internal conversion gives for K shell electrons having k = 1 the following internal conversion coefficient, $\alpha_1 \sim 10^{-4}$, $\beta_1 = 10^{-3}$ for Z = 33. (Sl.,Ba.,56). Here $k = E_\gamma/m_o c^2$, $\alpha_1 = N(K)/N(E1)$ and $\beta_1 = N(K)/N(M1)$. Internal conversion coefficients decrease rapidly with energy and are larger for higher multipolarity. Also as Z increases the internal conversion coefficient increases. The

above shows that transition intensities are the gamma ray intensities and that the former need no correction for internal conversion.

7.3 DETERMINATION OF A DECAY SCHEME

The proton capture results in a nuclear alignment which is achieved by particle absorption. The initial state is aligned but not polarized. As a consequence of this alignment the probability of emission of a gamma ray is angular dependent and the empirical dependence can be written as:

$$W_{exp.}(\theta) = \sum_k a_k Q_k P_k(\cos\theta) \qquad (6)$$

The a_k depend on quantities which charactarize the nuclear transition and on quantities describing the alignment of the initial nuclear state. The Q_k are attenuation coefficients due to finite size of detector. The Q_k depend on the geometry of the experimental set up and on the gamma ray absorption coefficient for the detector. The $P_k(\cos\theta)$ are the Legendre polynomials. If the initial state formed has definite parity then the sum is over even values of k. In practice the contribution from terms for

$k > 4$ is negligible. So that the expression used is:

$$W_{exp.}(\theta) = a_0 + a_2 Q_2 P_2(\cos\theta) + a_4 Q_4 P_4(\cos\theta) \qquad (7)$$

So that in principle in order to get the relative strength of given gamma rays one should average the intensity of each peak over several angles. The angular dependence of the gamma rays can be decreased by choosing an angle such that the generally predominant angular dependent term $a_2 Q_2 P_2(\cos\theta)$ vanishes. $P_2(\cos\theta)$ is zero for $\theta = 125^\circ$. So observing the gamma rays at 125° reduces the angular dependence and gives generally the relative strength of each gamma ray without having to average out over several angles.

Intensities of gamma rays were obtained from 125° spectra. Before trying to establish a decay scheme, possible gamma ray transition energies between previously reported values of energy levels of ^{59}Cu were found. The probable uncertainty in these values was about ± 19 kev. This also indicates all those gamma rays which may not resolved by the spectrometer. A branch of the decay is not regarded as established unless both the sum of the energies and the intensities

of the cascading gamma rays are consistent within the estimated experimental uncertainties.

8. RESULTS

8.1 CALCULATION OF PARTIAL WIDTHS

For radiative proton capture the nuclear reaction process is of the type:

$$a + X \rightarrow C^* \rightarrow Y + \gamma$$

where a is the incident particle, in this case a proton, X and Y are the target and residual nucleus and C* the compound nucleus. Letting i_1 denote the intrinsic spin of particle a and I_o the total angular momenta of the target nucleus and J_1 the corresponding quantity for the compound nuclear state formed in the interaction, the cross-section for the process can be written as:

$$\sigma(E) = \frac{\pi \lambda^2 (2J_1 + 1)}{(2i_1 + 1)(2I_o + 1)} \frac{\Sigma \Gamma_p \Gamma_\gamma}{(E - E_r)^2 + (\Gamma/2)^2} \qquad (8)$$

where Γ_p and Γ_γ are the widths for formation and decay respectively and the sum implies that all possible channel spins and orbitals are included in Γ_p and that all multipole mixtures are included in Γ_γ. E_r represents the resonant proton energy and λ is the center of mass wavelength of the incident particle. Γ is defined as:

$$\Gamma = \Gamma_p + \Gamma_\gamma \tag{9}$$

In practice one obtains the experimental cross-section by measuring the resonant gamma ray yield for a given resonance. The gamma ray yield from targets of finite thickness including effects of straggle can be written as:

$$y(E_a,t) = n \int_{x=0}^{t} \int_{E=-\infty}^{\infty} \int_{E_i}^{\infty} g(E_a,E_i)\, w\,(E_i,E,x)\, \sigma(E)\, dE\, dE_i\, dx \tag{10}$$

where n is the number of atoms per gram of the target, $\sigma(E)$ is the cross-section per atom in cm^2 at an energy E, $w(E_i,E,x)\,dE$ is the probability that a proton incident on the target with an energy E_i has an

energy between E and E + dE at a depth of x g/cm^2 in the target, $g(E_a,E_i)dE_i$ is the probability that a particle in the incident beam of mean energy E_a has an energy between E_i and $E_i + dE_i$ and t is the target thickness in g/cm^2. The integrals involving energy can be taken with a lower limit of $-\infty$ since σ, g, and w are all assumed to quickly vanish on both sides of their maximum values. Calculations, assuming certain dependence of σ, g, w and letting the thickness $t \to \infty$ (see En.,De.,59), to obtain the step in the thick target yield $y(\infty,\infty)$ gives:

$$y(\infty,\infty) = \frac{n}{k} \int_{-\infty}^{\infty} \sigma(E)\, dE \qquad (11)$$

$y(\infty,\infty)$ is a measure of the number of reactions per incident particle and n/k is the inverse stopping power of the target in units of energy times cm^2/atom it can easily be shown that:

$$\int_{-\infty}^{\infty} \sigma(E)\, dE = \frac{\lambda^2}{2} \frac{(2J_1 + 1)}{(2i_1 + 1)(2I_o + 1)} \frac{\Sigma\, \Gamma_p \Gamma_\gamma}{\Gamma} \qquad (12)$$

whence:

$$\frac{\Sigma\, \Gamma_p \Gamma_\gamma}{\Gamma} \frac{(2J_1 + 1)}{(2i_1 + 1)\,(2I_o + 1)} = \frac{2}{\lambda^2} \frac{k}{n}\, y(\infty,\infty) \qquad (13)$$

For protons incident on an even nucleus such as ^{58}Ni one as:

$$\frac{\Sigma\, \Gamma_p \Gamma_\gamma}{\Gamma} (2J_1 + 1) = \frac{4}{\lambda^2} \frac{k}{n}\, y(\infty,\infty) \qquad (14)$$

Arguments pertaining to the relative values of Γ_p and Γ_γ are given in (Bu.,Go.,57). They conclude that for resonances below 1.5 Mev, the assumption that $\Gamma_p >> \Gamma_\gamma$ breaks down at least for some resonances. Since all the resonances below 1.3 Mev are relatively weak it appears reasonable to assume that for most of these resonances $\Gamma_p < \Gamma_\gamma$. So that for all strong resonances between 1.3 Mev and 1.5 Mev and all resonances above 1.5 Mev equation (14) becomes:

$$\Sigma\, \Gamma_\gamma (2J_1 + 1) = \frac{4}{\lambda^2} \frac{k}{n}\, y(\infty,\infty) \qquad (15)$$

from which one can obtain the total gamma ray width if J_1, the spin of the resonant compound state, is known. This also requires a calculation of the center of mass wavelength of the incident proton, a knowledge of the stopping power and a knowledge of the number of reactions per incident proton.

The number of reactions that occured may be calculated by making use of the fact the ^{59}Cu resulting from the proton capture on ^{58}Ni is β^+ active with a half life of 80 seconds. 10.9% of the β^+ decays populate the 1303 kev level of ^{59}Ni while 7.8% of the β^+ decays populate the 878 kev level. Both levels decay by gamma ray emission to the ground state. Thus the number of reactions N*, i.e. the number of ^{59}Cu nucleus formed, is given by:

$$N^* = \frac{I(1303) \times 100}{\varepsilon(1303) \times 10.9} = \frac{I(878) \times 100}{\varepsilon(878) \times 7.8} \qquad (16)$$

where I stands for the number of counts in the integrated peak and ε stands for the absolute full energy peak efficiency for that given energy. The number of protons corresponding to N*, for a given resonance,

was measured by a current integrator.

The protons incident on the target produce secondary electrons which may result in an over estimation of the current. To prevent this one must apply a suppressor bias in order to prevent electrons leaving the target. However this was not done when the spectra were obtained and used for the partial width calculation. More information on the effect due to secondary electron emission was obtained from further measurements made on the 1424 and 1844 kev resonances with another thick target in a different target chamber. This time a suppressor bias of -300 volts was applied. This bias would have been sufficient to repel all secondary electrons see (Kr.,Ni.,Ba.,61). Unfortunately analysis of the data indicated that even before beginning accumulation of the spectra a short circuit had rendered the suppressor bias ineffective. In spite of the different geometry the measurements of $y(\infty,\infty)$ for both the 1424 and the 1844 kev resonances repeated within 25%. In order to correct the measured current, $I_{meas.}$, the data on secondary electron emission for H_1^+ ions normally incident on conditioned thick targets of Ni obtained by

B. Aarset et al. (Aa.,Cl.,Tar.,54) was used. A smooth curve drawn through their data points gave the true value of proton current, $I(H_1^+)$, for the different resonant proton energies studied, see figure 8.1a. The word conditioned used above means that the target was subject to a period of bombardment before any charge collection measurements were performed. This conditioning period is essential. Contamination and adsorbed gases increase secondary electron emission and must be minimized. Hence the nature of the target surface is critical. The conditioning period was found by B. Aarset et al. to be two to three hours with several microamperes of current. The fact that the measurements of $y(\infty,\infty)$ repeated within 25% indicates that targets were well conditioned and that secondary electron emission from ^{19}F contamination was not that important. However the correction due to this contaminant introduces an unknown uncertainty into the calculations in which the value of $y(\infty,\infty)$ is used. As can be seen from spectra (see section 8.2) several gamma ray peaks can be identified as due to proton capture on Cu and Zn isotopes. This obviously indicates an additional uncertainty in the number of protons hitting

figure 8.1a

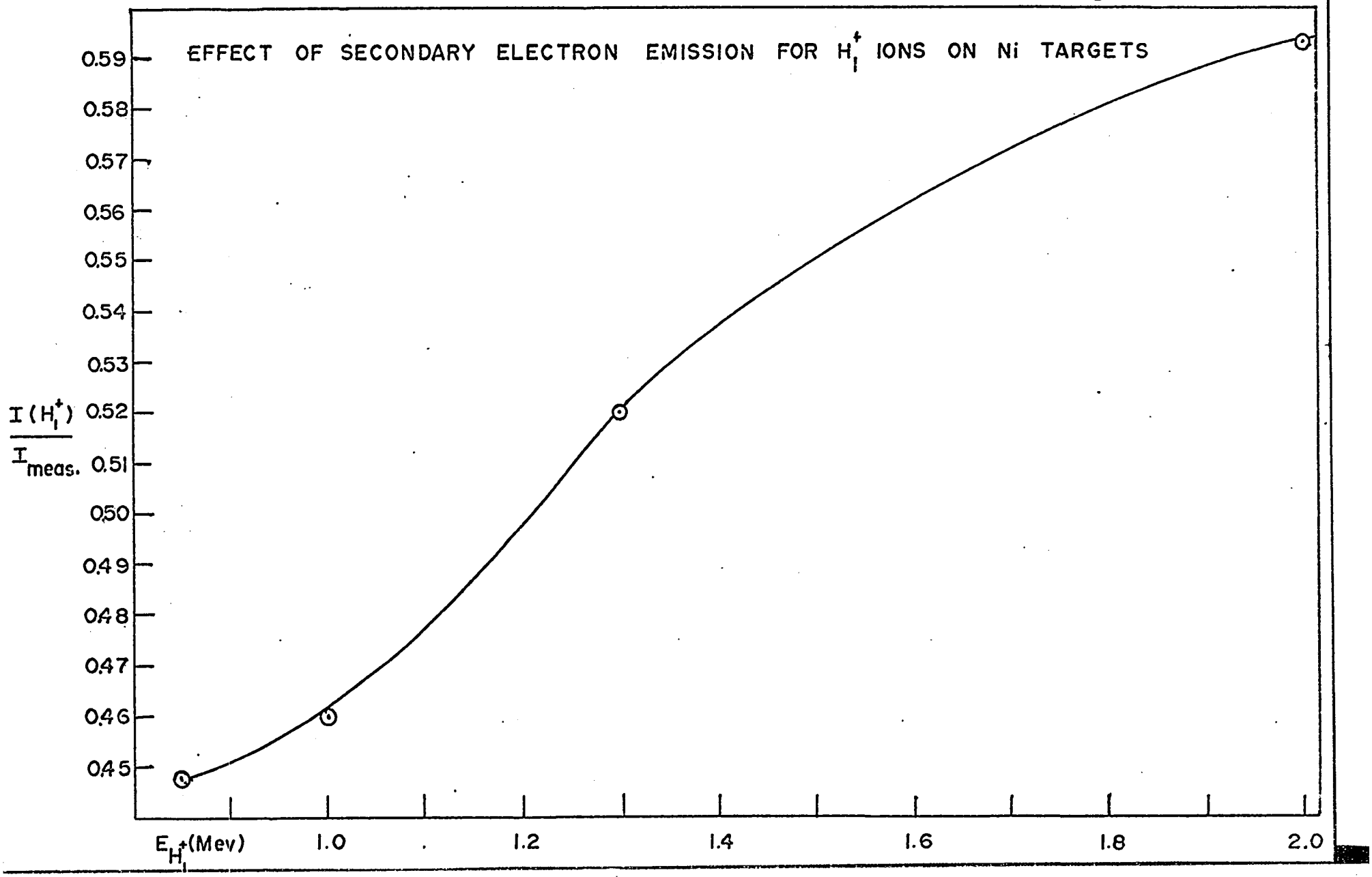
EFFECT OF SECONDARY ELECTRON EMISSION FOR H_1^+ IONS ON Ni TARGETS
0.59
0.58
0.57
0.56
0.55
0.54
0.53
0.52
0.51
0.50
0.49
0.48
0.47
0.46
0.45
$\frac{I(H_1^+)}{I_{meas.}}$
$E_{H_1^+}$(Mev)
1.0
1.2
1.4
1.6
1.8
2.0

the target. The first spectrum obtained for the 1424 kev resonance is one of those and yet the repeated resonance which did not have these peaks gave a value for the step in the thick target which is in agreement within 25% of the previously established value. Out of the 25% uncertainty, 12% can be attributed to measurement of N*, thus indicating an uncertainty of about 13% in the measurements of $I(H_1^+)$.

Shown in table 8.1a are the calculated integrated cross-section which are compared with the previous estimation of Butler and Gossett. Comparison of the results show in several cases a descrepancy larger than a factor of two, which was the estimated uncertainty of Butler and Gossett. The resulting partial gamma ray widths are given in the table. A spin between parentheses indicates that it is not fully established but is suggested tentatively from the decay of the resonance levels as discussed in the subsections of section 8.2. These spins are assumed in order to obtain an order of magnitude for the values of the partial gamma ray widths. The experimental partial gamma ray width for some transitions is given in Weisskopf units in table 8.1b. The average value of $|M|^2$ for transitions shown is 0.04 W.U. which

table 8.1a

E_p (kev)	Spin	± 25 % $\int\sigma(E)\,dE$ (ev barn/atom) Present Work	± factor of 2 $\int\sigma(e)\,dE$ (ev barn/atom) Butler & Gossett	Γ_γ(ev)
947	1/2	0.142	0.14	≥ 0.154
1100	(5/2)	0.500	0.05	(≥ 0.417)
1376	3/2	0.198	0.19	0.0321
1424	3/2	0.179	1.7	0.302
1716	3/2	0.0835	0.35	0.0169
1833	(7/2)	0.0143	0.063	(0.00157)
1844	1/2	0.759	2.1	0.334
1883	(3/2)	0.0451	--	(0.0102)
1923	(3/2)	0.234	--	(0.0544)

tabe 8.1b

E_p(kev)	Transition	Type	$\|M\|^2$
947	$E_x \rightarrow 0.492$	'M1	$\geq 1.55 \times 10^{-2}$
1376	$E_x \rightarrow 0.492$	*M1	0.902×10^{-2}
1424	$E_x \rightarrow 0$	*M1	4.63×10^{-2}
1424	$E_x \rightarrow 0.492$	*M1	9.32×10^{-2}
1716	$E_x \rightarrow 0$	'M1	0.31×10^{-2}
1844	$E_x \rightarrow 0$	*M1	10.03×10^{-2}

' indicates most favored type
* indicates favored established dipole

may be compared with Wilkinson's most probable speed of 0.15 Weisskopf unit (Wi.,56) for magnetic dipole transitions in light nuclei ($A < 20$) with a spread of a factor of twenty either way. The radiative widths calculated by Weisskopf assume one particle of spin J making a trasition in an infinitely massive and uncharged potential well and ending in a final state of zero orbital angular momentum. Because of this simplified model it is expected that observed transitions strengths will vary widely relative to Weisskopf's single particle strength estimates.

Values of $|M|^2$ greater than unity usually indicate collective effects which tend to enhence the speeds of transitions since for collective effects we must multiply the one particle matrix representing the transition by the number of particles needed for a full specification of the states between which the transition takes place.

8.2 BRANCHING RATIOS

Branching ratios for the 947, 1100, 1376, 1424, 1716, 1833, 1844, 1883 and 1923 resonances of the $^{58}Ni\ (p,\gamma)\ ^{59}Cu$ reaction have been determined from 125^{o} spectra obtained with the Ge(Li) detector. The

decay of some of these can be compare with previous $^{58}Ni\ (p,\gamma)\ ^{59}Cu$ work.

8.2a THE 947 KEV RESONANCE (E_x = 4.350 Mev)

The spectrum at 125° of the 947 kev resonance is shown in figure 8.2a. Table 8.2a gives the data obtained from the 947 kev spectra and the resulting decay for the resonance level is shown in the summary figure which is figure 8.2k. The decay of the resonance level populates a 1837 kev level which is probably that observed previously only in the $^{58}Ni\ (d,n)\ ^{59}Cu$, see (Ma.,St.,67), while the $^{58}Ni\ (^3He,d)\ ^{59}Cu$ stripping reaction has not populated that level, see (Pu.,Ro.,Ho.,67). All non-background gamma rays are accounted for.

8.2b THE 1100 KEV RESONANCE (E_x = 4.500 Mev)

The spectrum at 125° of the 1100 kev resonance is shown figure 8.2b. The data of the analysed spectra is shown in table 8.2b and the resulting consistent decays scheme shown in figure 8.2k. Three branches have been established: a strong ground state transition and two weak branches to the first excited level and to the 2263 kev level. The strong branch to ground suggests a spin of 3/2 or 5/2 for the resonance level. In tables of data for each resonance a star against a gamma ray energy indicates an unexplained non-background gamma ray and given in the transition column corresponding

^{58}NI (P,Y) ^{59}CU
947 KEV RESONANCE 125 DEGREE SPECTRUM (2 HOURS AT 10 MICROAMPS) figure 8.2a

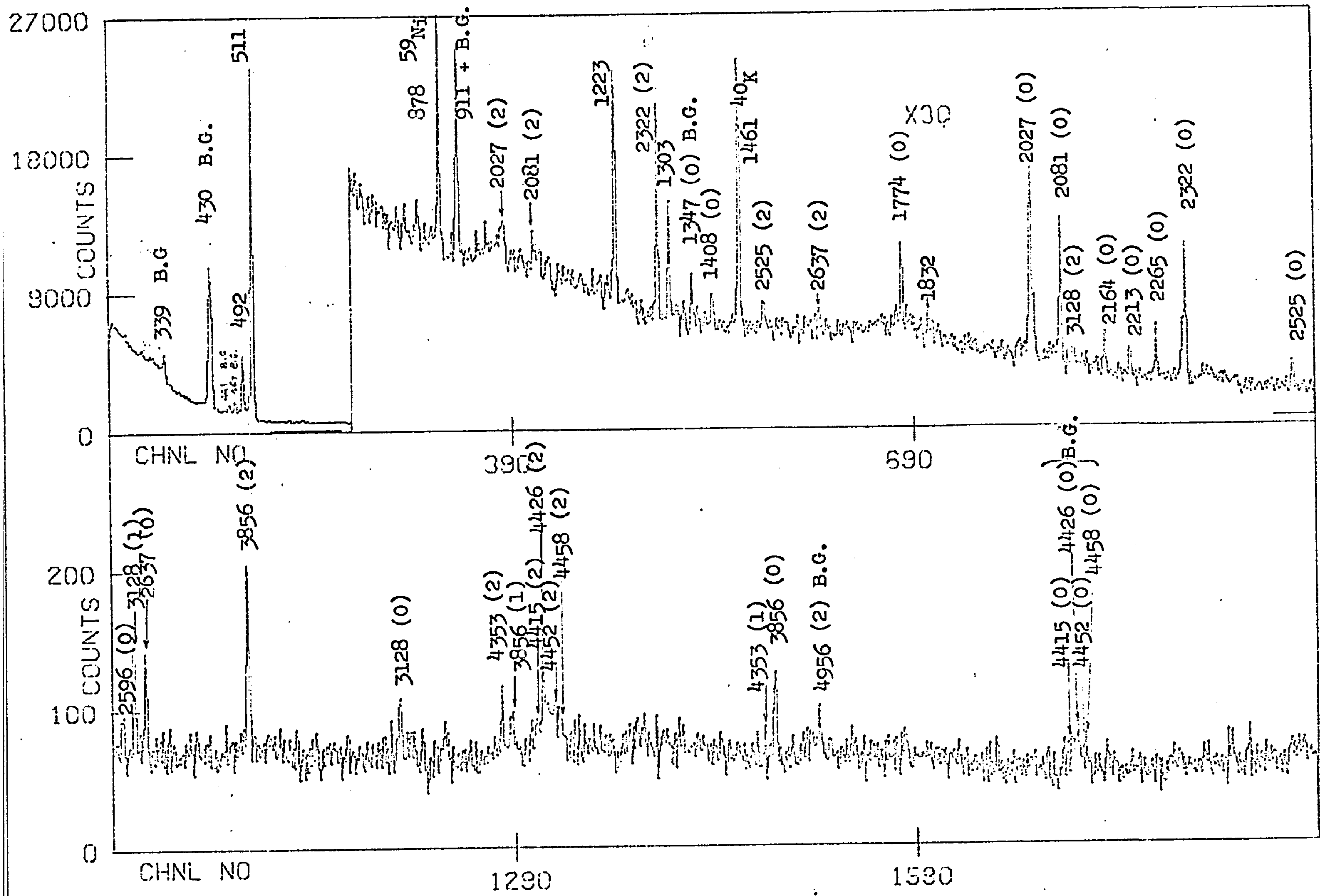

E_p = 947 kev , E_x = 4351 kev

table 8.2a

TRANSITION	E_γ(kev) ± 3 kev	INTEGRATED COUNTS	I (intensity) $\times 10^{-6}$	ΔI %
E_x → 0	4353	120 (2)	0.970	±18
E_x → 491	3856	128 (0)	0.985	± 15
491 → 0	492	--	--	± --
E_x → 1837	2525	141 (0)	0.635	± 15
1837 → 0	1832	120 (0)	0.343	± 15
E_x → 2263	2081	538 (0)	1.86	± 12
2263 → 0	2265	175 (0)	0.674	± 15
2263 → 491	1774	332 (0)	0.921	± 15
E_x → 2319	2028	1051 (0)	3.51	± 8
2319 → 0	2322	711 (0)	2.85	± 10
2319 → 911	1408	151 (0)	0.314	± 15
E_x → 3128	1223	955 (0)	1.69	± 8
3128 → 0	3128	107 (0)	0.630	± 15
3128 → 491	2637	125 (0)	0.586	± 15
3128 → 911	2213	127 (0)	0.439	± 15
911 → 0	911	841 (0)	1.11	± 15
	* 467	900 (0)	--	
	* 441	480 (0)	--	
	* 2596	60 (0)	0.262	±

58NI (P,Y) 59CU
1100 KEV RESONANCE 125 degree SPECTRUM (2 HOURS AT 45 MICROAMPS)
COUNTS
CHNL NO
509
610
671
833
880
912
963
991 B.G.
1035
1070
1108
1120
1138
1154
1290 B.G.
1369 B.G.
1461
40K
01X
1532
1634 B.G.
1776 B.G.
1972
2160
2205
2263
2320
2608 B.G.
4441
4965
4244 (2) + B.G.
4418 (2)
4431 (2)
4452 (2)
4460 (2)
4497 (2)
3491
4244 (1) + B.G.
4497 (1)
4005 (0)
4244 (0)
4418 (0)
4431 (0)
4452 (0)
4460 (0)
4497 (0)
B.G.
19F6129 (2)
COUNTS
CHNL NO

figure 8.2b

E_p = 1100 kev , E_x = 4500 kev

table 8.28

TRANSITION	E_γ (kev) ± 3 kev	INTEGRATED COUNTS	I (intensity) x10^{-6}	ΔI %
E_x → 0	4497	397 (0)	3.71	± 7
E_x → 491	4005	63 (0)	0.511	± 15
491 → 0	491	3870 (0)	---	-
E_x → 2263	2230	140 (0)	0.532	± 13
2263 → 0	2263	100 (0)	0.385	± 13
	* 610	550 (0)	0.406	± 30
3040 → 2369	* 671	379 (0)	0.324	± 15
	* 833	180 (0)	0.212	± 15
	* 963	230 (0)	0.324	± 15
	*1035	125 (0)	0.910	± 15
3040 → 1964	*1070	95 (0)	0.153	± 15
	*1108	90 (0)	0.151	± 15
	*1120	150 (0)	0.252	± 20
	*1138	215 (0)	0.371	± 20
3128 → 1964	*1154	310 (0)	0.541	± 20
	*1532	236 (0)	0.547	± 15
	*1972	140 (0)	0.425	± 15
2269 → 491	*2205	160 (0)	0.551	± 15

to each unexplained gamma ray energy is given a possible source of that gamma ray. Eight of the unexplained gamma rays of table 8.2b correspond to gamma ray energies obtainable from radiative proton capture on Cu and Zn isotopes while only four correspond to energy differences between the known levels of ^{59}Cu up to an energy of excitation of 3128 kev as shown in table 8.2b. A most probable explanation is that for the off resonance spectrum the proton beam was well focussed on the target while for the on resonance run the beam was not so well focussed on the target and was hitting the brass target chamber hence giving rise to gamma rays which did not appear in the off resonance spectra and as such could not be identified as background gamma rays.

8.2c THE 1376 KEV RESONANCE (E_x = 4.767 Mev)

The 125° spectrum of the 1376 kev resonance is shown in figure 8.2c. The data of the analysed spectra are given in table 8.2c. Figure 8.2c' compares the results of the present work with the previous ^{58}Ni (p,γ) ^{59}Cu work of Butler and Gossett (Bu.,Go.,57). The dashed line with strength [2] indicates that a transition to the 1383 kev level is not observed in the

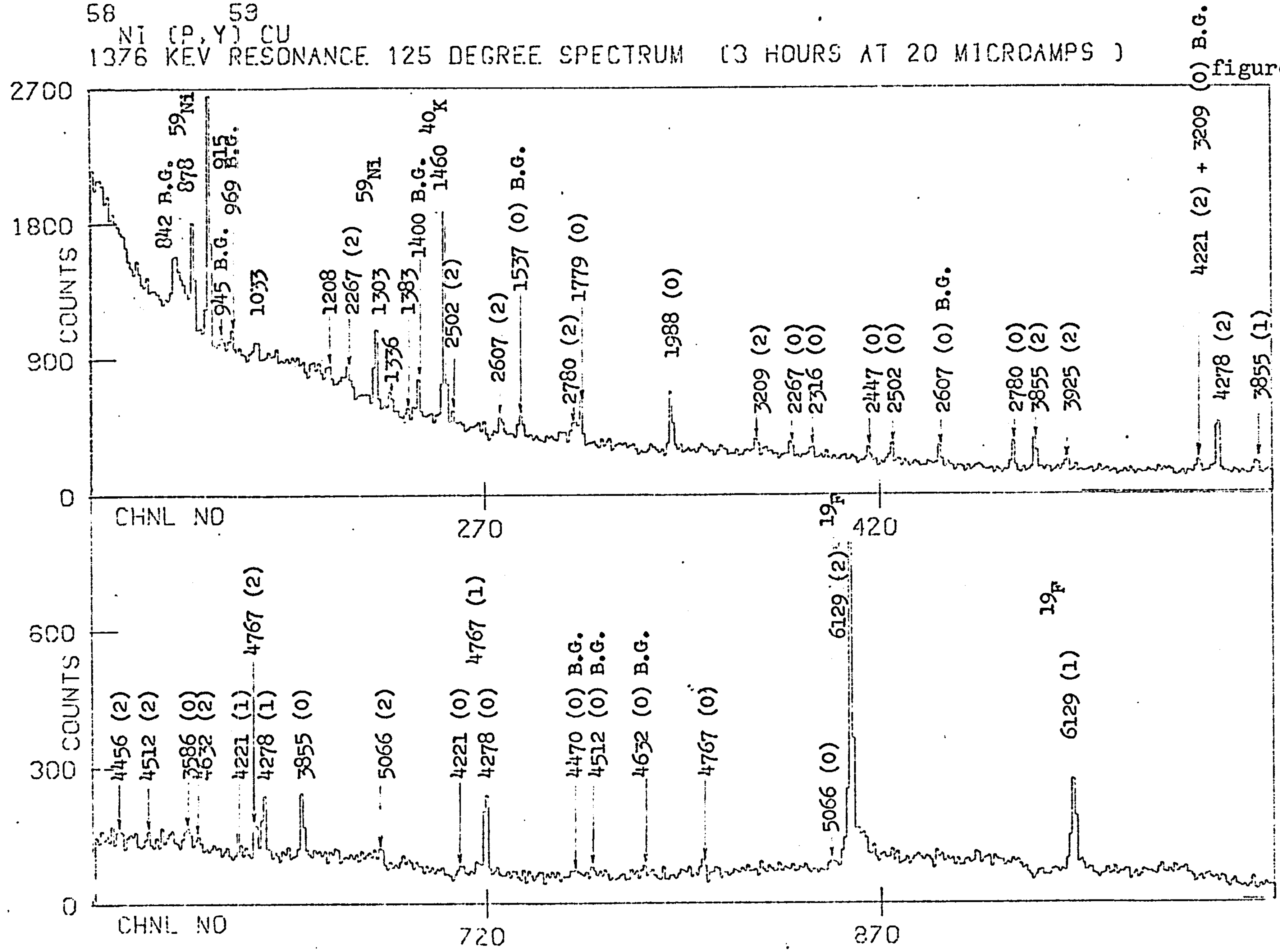
58 NI (P,Y) 59 CU
1376 KEV RESONANCE 125 DEGREE SPECTRUM (3 HOURS AT 20 MICROAMPS)
2700
1800
900
0
COUNTS
CHNL NO
270
420
842 B.G.
878
59Ni
915
945 B.G.
969 B.G.
1033
1208
2267 (2)
1303
59Ni
1336
1383
1400 B.G.
1460
40K
2502 (2)
2607 (2)
1537 (0) B.G.
2780 (2)
1779 (0)
1988 (0)
3209 (2)
2267 (0)
2316 (0)
2447 (0)
2502 (0)
2607 (0) B.G.
2780 (0)
3855 (2)
3925 (2)
4221 (2) + 3209 (0) B.G.
4278 (2)
3855 (1)
19F
600
300
4456 (2)
4512 (2)
3586 (0)
4632 (2)
4221 (1)
4767 (2)
4278 (1)
3855 (0)
5066 (2)
4221 (0)
4278 (0)
4767 (1)
4470 (0) B.G.
4512 (0) B.G.
4632 (0) B.G.
4767 (0)
5066 (0)
6129 (2)
6129 (1)
720
870

figure 8.2c

E_p = 1376 kev, E_x = 4773 kev

table 8.2c

TRANSITION	E_γ(kev) ± 4 kev	INTEGRATED COUNTS	I (intensity) $\times 10^{-6}$	ΔI %
E_x → 0	4767	70 (0)	0.700	± 15
E_x → 491	4278	334 (0)	2.95	± 8
491 → 0	491	--	--	--
E_x → 911	3855	222 (0)	1.71	± 12
911 → 0	915	2449 (0)	3.26	± 15
E_x → 1988	2780	270 (0)	1.35	± 13
1988 → 0	1988	515 (0)	1.51	± 10
E_x → 2319	2447	156 (0)	0.621	± 15
2319 → 0	2317	138 (0)	0.512	± 15
E_x → 2263	2502	213 (0)	0.891	± 15
2263 → 0	2267	179 (0)	0.640	± 15
2263 → 492	1779	280 (0)	0.700	± 35
1383 → 0	1383	100 (0)	0.210	± 15
	*1033	160 (0)	0.242	± 15
3040 → 1836	*1208	150 (0)	0.329	± 15
1836 → 491	*1336	200 (0)	0.400	± 10

E_p=1.376 kev figure 8.2c'

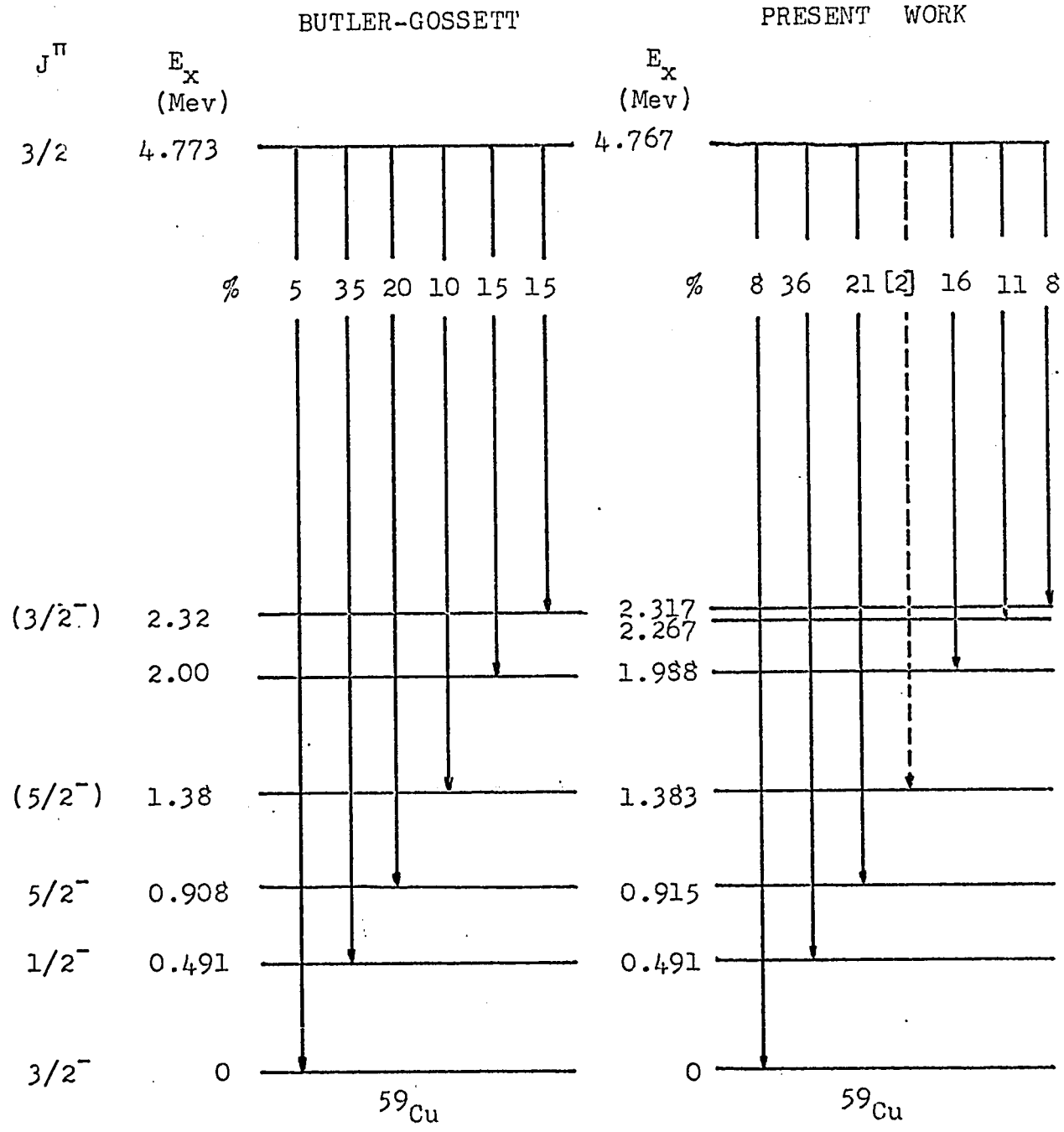

BRANCHING RATIOS OF RESONANCE LEVEL

125^{o} spectrum and is less than 2% of the total decay. Butler and Gossett estimate their uncertainties in the branching ratios to be ± 10% of the total decay while a maximum uncertainty of 15% in each branch of the decay is estimated for the present work. The transition to a 2.00 Mev level determined by Butler and Gossett is most probably the transition to the 1.988 Mev level of the present work. The uncertainty in the energy levels found is ± 4 kev, while in the previous work done with a NaI (Tl) detector an uncertainty of ± 20 kev is quoted. Although the primary gamma ray (or rays) feeding the possible 1383 kev level was not observed, the 1383 kev gamma ray is exceptionnally listed as a gamma ray of the decay corresponding to a transition between the 1383 kev level and the ground state of ^{59}Cu. This exception was made since the level was previously reported to be populated by this resonance by Butler and Gossett and in addition the 90^{o} spectrum of this resonance showed a weak peak having the same energy as that of the primary gamma ray feeding the 1383 kev level from the excited state. Even though the cascade is consistent in energy within experimental uncertainties the consistency in the intensity could not be checked

because of unknown attenuation effect at this angle. Three other unexplained non-background gamma rays are listed, two of which correspond to energy differences between known levels of ^{59}Cu up to an excitation energy of 3128 kev. The necessary primary gamma ray feeding the 3040 kev level is not observed so that the origin of the gamma ray leaving the 3040 kev level and the gamma ray in cascade with it are classified as unexplained.

8.2d THE 1424 KEV RESONANCE (E_x = 4.817 Mev)

The 125° spectrum for 1424 kev resonance is shown in figure 8.2d and the analysed spectra tabulated in table 8.2d. A comparison with previously established decay of the resonance level is given in figure 8.2d'. The transitions to the 1383 and 2319 levels are not observed but are both less than 1% of the total decay. The secondary gamma ray from the most probable 1383 kev level to ground was however observed. Additional transitions have been observed to the second excited level and to the 1988 kev level. The two most intense lines are to ground and to the first excited state. Four unexplained non-background gamma rays are listed in table 8.2d and their possible origin from transitions between the known levels of ^{59}Cu are given.

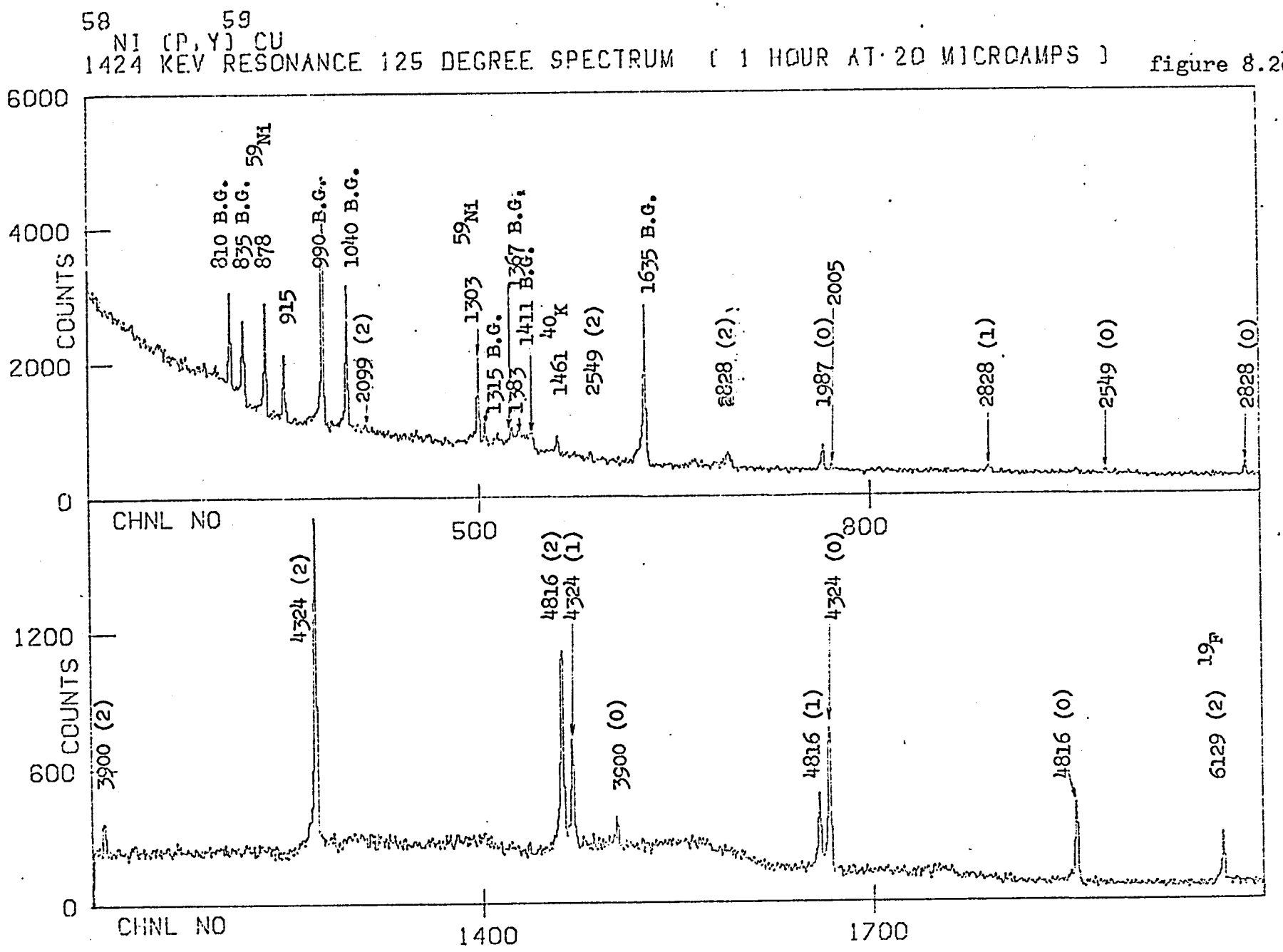
58 59
NI (P,Y) CU
1424 KEV RESONANCE 125 DEGREE SPECTRUM (1 HOUR AT 20 MICROAMPS)
6000
4000
2000
0
COUNTS
CHNL NO
500
800
310 B.G.
835 B.G.
878
59Ni
915
990 B.G.
1040 B.G.
2099 (2)
59Ni
1303
1315 B.G.
1383
1411 B.G.
1461 40K
2549 (2)
1635 B.G.
1987 (0)
2005
2828 (1)
2549 (0)
2828 (0)
1200
600
0
COUNTS
CHNL NO
1400
1700
3900 (2)
4324 (2)
4816 (2)
4816 (1)
4324
3900 (0)
4816 (1)
4324 (0)
4816 (0)
19F
6129 (2)

figure 8.2d

E_p = 1424 kev , E_x = 4820 kev

table 8.2d

TRANSITION	E_γ (kev) ± 3 kev	INTEGRATED COUNTS	I (intensity) $\times 10^{-7}$	ΔI %
Ex → 0	4816	799 (0)	0.815	± 9
E_x → 491	4324	1680 (0)	1.49	± 7
491 → 0	491	--	--	
Ex → 911	3900	307 (0)	0.249	± 10
911 → 0	915	1800 (0)	0.240	± 11
E_x → 1988	2828	350 (0)	0.180	± 8
1988 → 0	1987	809 (0)	0.216	± 10
1383 → 0	1383	400 (0)	0.080	± 30
	*2754	96 (0)	0.048	± 15
3040 → 491	*2549	160 (0)	0.069	± 15
2913 → 911	*2005	190 (0)	0.057	± 15
	*2099	152	0.046	± 15

E_p = 1.424 Mev figure 8.2d'

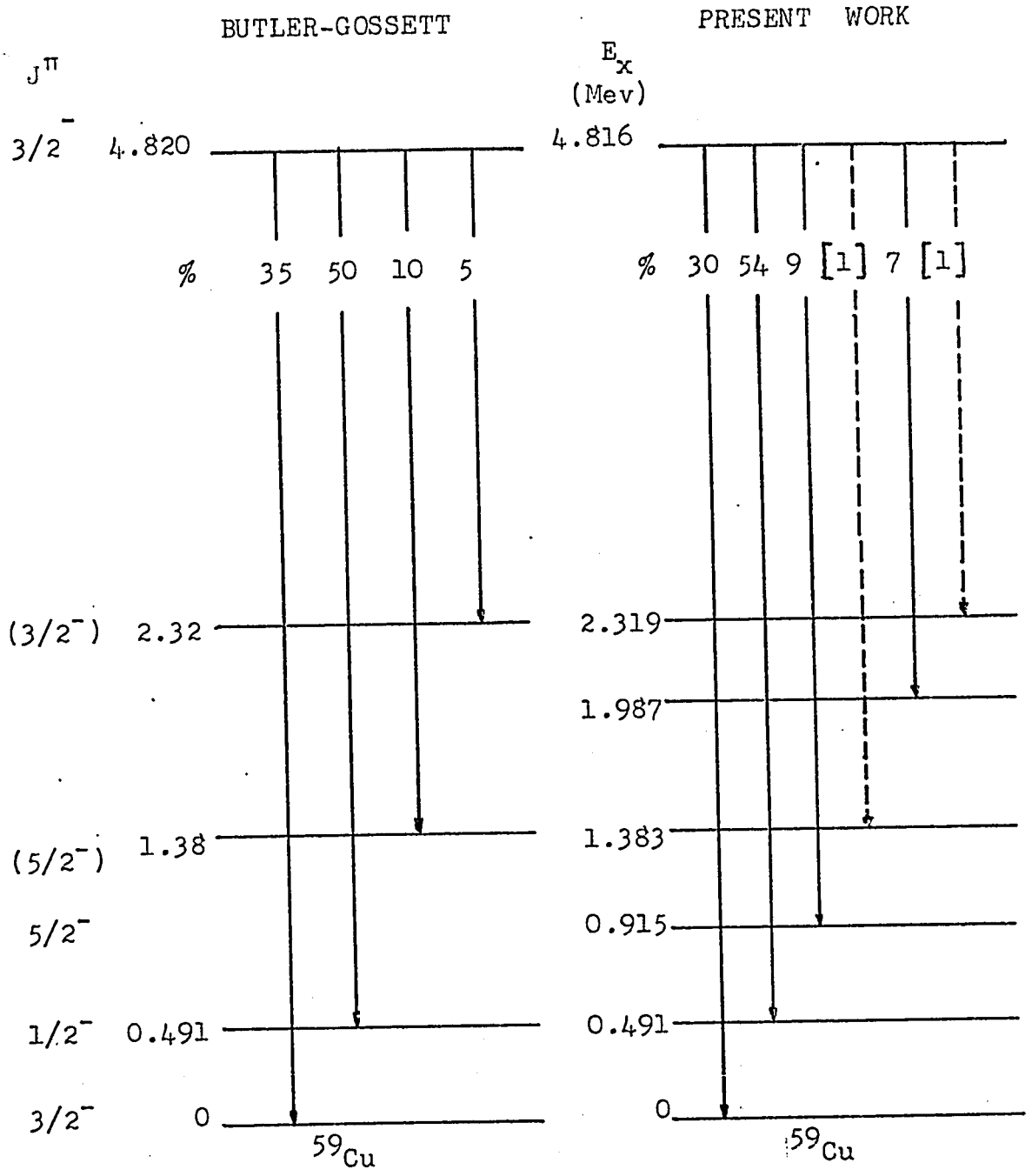

BRANCHING RATIOS OF RESONANCE LEVEL

8.2e THE 1716 KEV RESONANCE (E_x = 5.107 Mev)

Figure 8.2e shows the 125° spectrum. Table 8.2e lists the data after analysis of the spectra for this resonance and figure 8.2e' gives a comparison with the previous study. A transition to the 2319 kev level is not observed and is less than 2% of the total decay. Again two additional branches have been observed; to the first excited state and the 1988 kev level. The most intense two lines are to ground and to the second excited level. The 1988 kev gamma previously observed in the 1376 and 1424 kev resonances shows a strong angular dependence. It's intensity is approximately 80 integrated counts at 125° increasing to 290 integrated counts at 90° for the same charge collection. A descrepancy of 17% in the intensity between the primary gamma ray feeding the 1988 kev level from the resonance level and the intensity of the secondary gamma ray leaving the 1988 kev level and going to ground is observed. There are three unexplained non-background gamma rays, only one of which corresponds to three possible transitions between known levels of ^{59}Cu. The three transitions are: 3128 → 2263, 2699 → 1837 and 2263 → 1394.

58 Ni + Cr, Y) Cu
1715 KEV RESONANCE 125 DEGREE SPECTRUM (2 HOURS AT 25 MICROAMPS)
COUNTS
CHNL NO
740 B.G.
788 B.G.
864
877 59Ni
915
1011
1303 59Ni
1370 B.G.
1460 40K
1634 B.G.
1707
1988
2155
3525 (2)
3525 (1)
3115 (0)
4191 (2)
4290 (2)
3525 (0) B.G.
4615 (2)
4191 (1)
4615 (1)
5107 (2)
4191 (0)
4290 (0) B.G.
4615 (0)
5107 (1)
5107 (0) + 6129 (2) 19F
6129 (1) 19F
270
420
720

Figure 8.2e

E_p = 1716 kev , E_x = 5107 kev

table 8.2a

TRANSITION	E_γ (kev) ± 4 kev	INTEGRATED COUNTS	I (intensity) x10^{-6}	ΔI %
E_x → 0	5107	211 (0)	2.38	± 8
E_x → 491	4615	72 (0)	0.705	± 8
491 → 0	490	--	--	
E_x → 911	4190	218 (0)	1.89	± 8
911 → 0	915	1800 (0)	2.40	± 6
E_x → 1988	3115	100 (0)	0.566	± 8
1988 → 0	1988	80 (0)	0.220	± 8
three possibilities	* 864			
	*1011			
	*1707			
	*2455			

E_p = 1.716 Mev figure 8.2e'

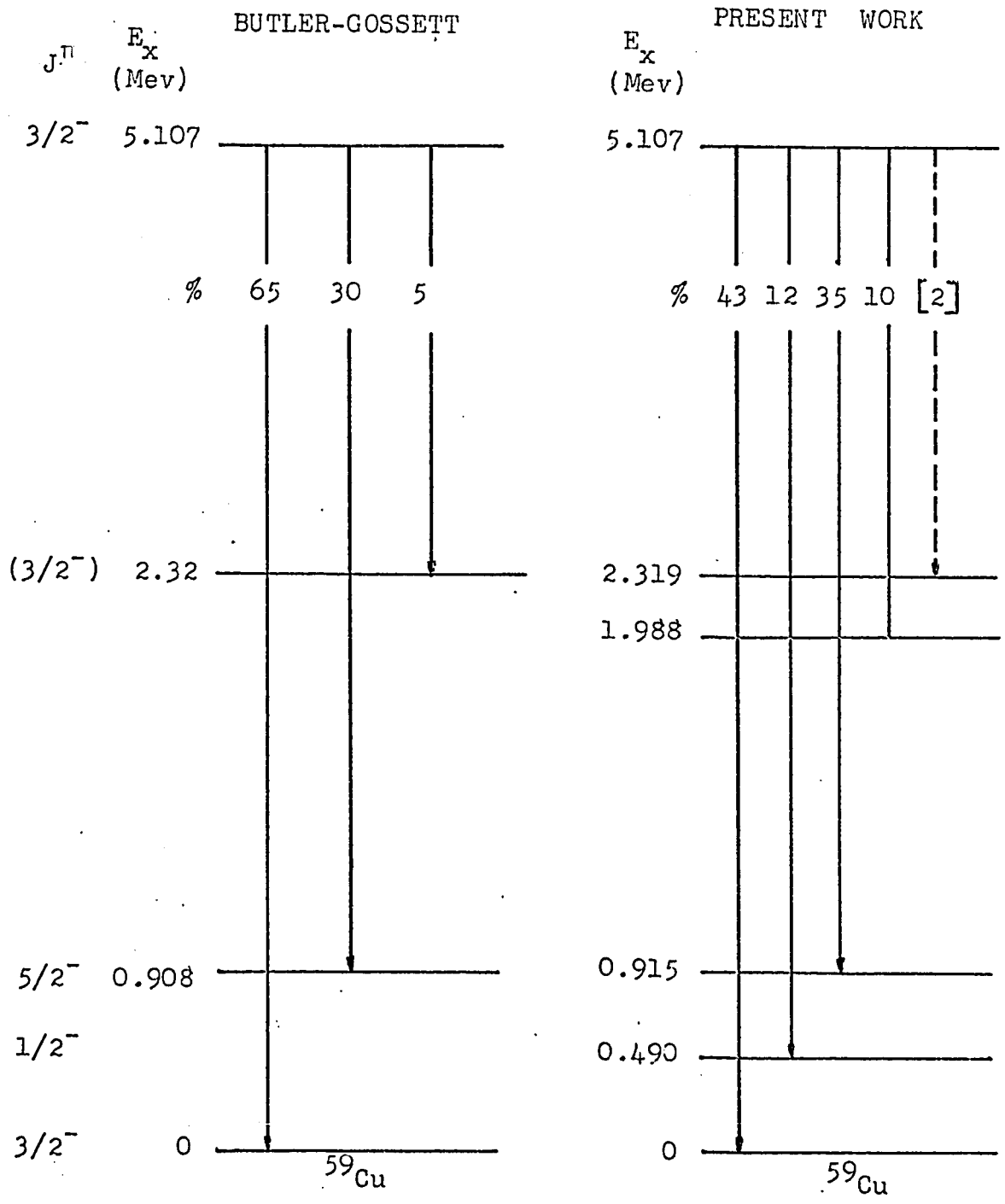

BRANCHING RATIOS OF RESONANCE LEVEL

8.2f THE 1833 KEV RESONANCE (E_x = 5.222 Mev)

The spectrum at 125° is given in figure 8.2f and the analysed data obtained from the spectra of this resonance listed in table 8.2f. The resulting decay scheme is given in the summary of figure 8.2k. There is evidence of a 1398 kev level. Two gamma rays of energy of 914 and 3627 kev indicate that the 914 and the 3627 kev levels are populated. The intensity of the primary gamma ray feeding the 4533 kev level is three times smaller than the intensity of the cascading gamma ray going to ground. Since this is unlikely it can only be said that the 4533 kev level is populated by this resonance. However it is impossible to fit them into a consistent decay scheme. The 914 level is not mainly fed directly from the resonance level since no indication of the primary gamma ray leaving the resonance level is observed even with an expected observable second escape peak intensity (approximately 80 counts) if population occured only from the resonance level. The primary gamma ray feeding the 3631 kev level is also unobserved even with an expected strong intensity (approximately 280 counts) of the full energy peak.

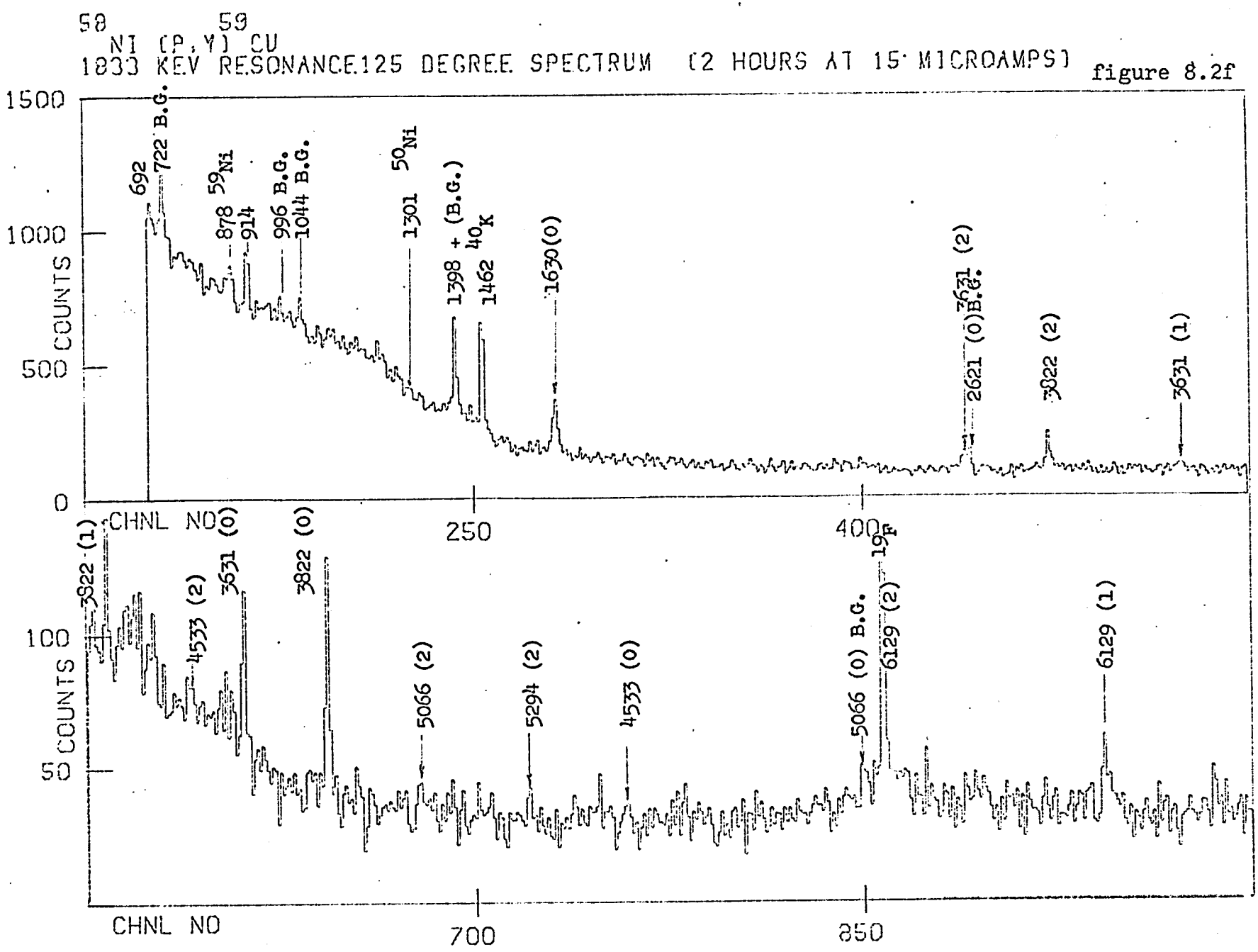
58 59
NI (P,Y) CU
1033 KEV RESONANCE.125 DEGREE SPECTRUM (2 HOURS AT 15 MICROAMPS)
1500
1000
500
0
COUNTS
692
722 B.G.
878
59Ni
914
996 B.G.
1044 B.G.
1301
50Ni
1398 + (B.G.)
40K
1462
1630(0)
2621 (0)
3631 (2)
B.G.
3822 (2)
3631 (1)
CHNL NO
250
400
100
50
COUNTS
3822 (1)
4533 (2)
3631 (0)
3822 (0)
5066 (2)
5294 (2)
4533 (0)
5066 (0) B.G.
19F
6129 (2)
6129 (1)
CHNL NO
700
850

figure 8.2f

E_p = 1833 kev , E_x = 5222 kev

table 8.2f

TRANSITION	E_γ (kev) ± ¼ kev	INTEGRATED COUNTS	I (intensity) x10^{-6}	ΔI %
E_x → 1398	3822	135 (0)	1.04	± 15
1398 → 0	1398	540 (0)	1.16	± 10
E_x → 4530	692	124 (0)	0.0961	± 25
4530 → 0	4533	35 (0)	0.330	± 25
911 → 0	* 914	400 (0)	0.530	± 15
3627 → 0	*3631	85 (0)	0.611	± 15

The number of integrated counts listed in table 8.2f for E_γ = 1398 kev could possibly have a background contribution of approximately 25% since a gamma ray of this energy appeared in the background spectrum which was taken approximately 15 kev above the 1844 kev resonance. However this background gamma ray did not appear in the 1844 kev resonance and since the 1844 and 1833 kev resonances are only 11 kev apart the 1398 kev gamma ray would be expected to appear in both the 1833 and 1844 spectra. Further the consistency in the intensity and energy of the cascade is good. In summary there is substantial evidence for the existence of a new level at 1398 kev. Independent experimental evidence for the existence of a close doublet at this excitation energy was obtained by Blair (Bl.,64). Because the resonance is weak and does not decay to any of the known lower 5/2 levels the spin of the resonance level is expected to be high, probably 7/2 or higher.

8.2g THE 1844 KEV RESONANCE (E_x = 5.233 Mev)

A consistent decay scheme of the 1844 kev resonance level is shown in figure 8.2g' while the spectrum at 125° and the tabulated data are given in figure 8.2g

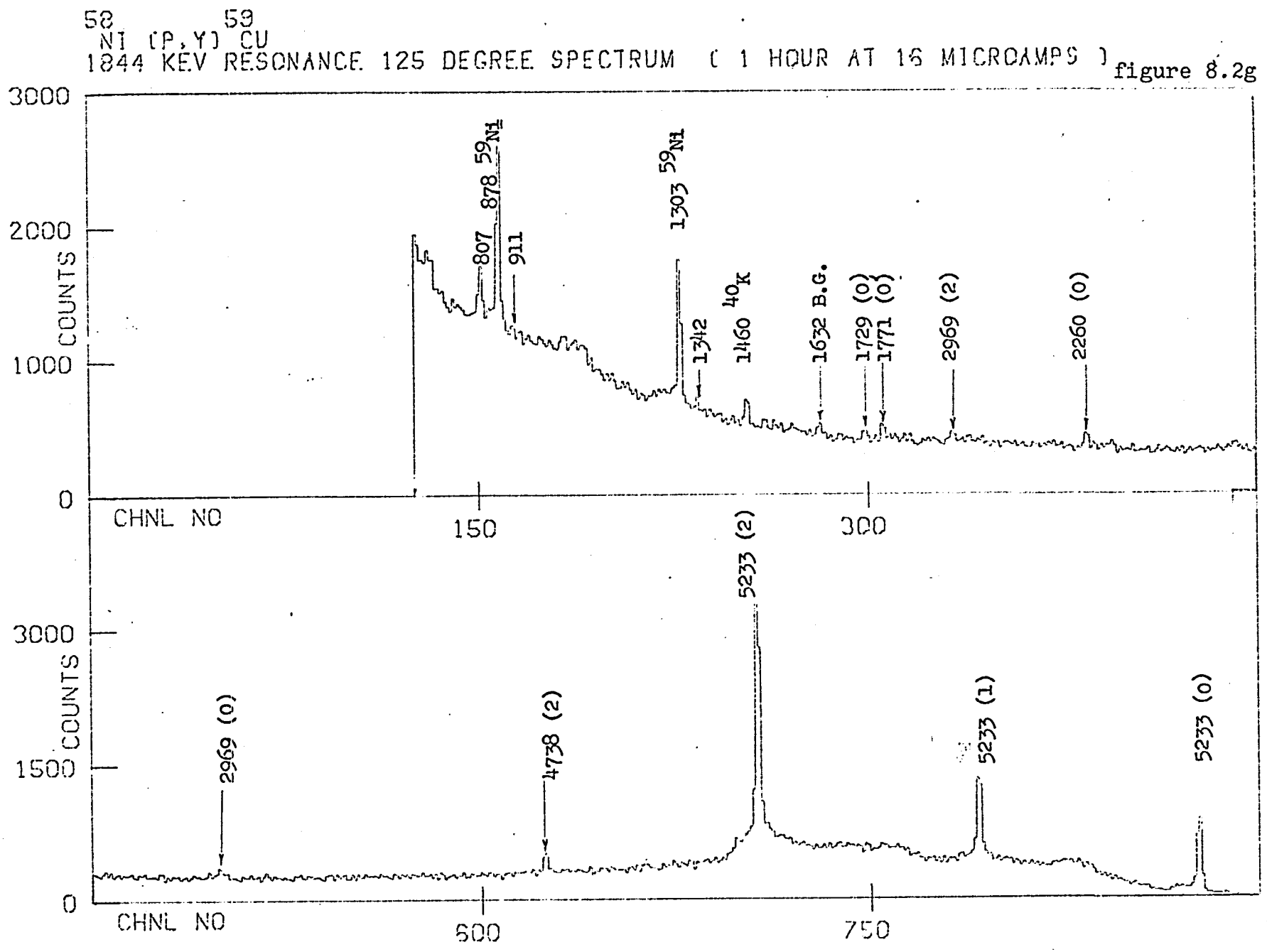
58 59
NI (P,Y) CU
1844 KEV RESONANCE 125 DEGREE SPECTRUM (1 HOUR AT 16 MICROAMPS)
3000
2000
1000
0
COUNTS
CHNL NO
150
300
807
878
59Ni
911
1303
59Ni
1342
40K
1460
1632 B.G.
1729 (0)
1771 (0)
2969 (2)
2260 (0)
3000
1500
0
COUNTS
CHNL NO
600
750
2969 (0)
4738 (2)
5233 (2)
5233 (1)
5233 (0)

figure 8.2g

E_p = 1844 kev , E_x = 5233 kev

table 8.2g

TRANSITION	E_γ(kev) ± 4 kev	INTEGRATED COUNTS	I (intensity) $\times 10^{-7}$	ΔI %
E_x → 0	5233	1670 (0)	1.92	± 7
E_x → 491	4738	140 (2)	0.0536	± 17
491 → 0	491	--		
E_x → 2263	2969	185 (0)	0.103	± 15
2263 → 0	2260	200 (0)	0.0731	± 15
2263 → 491	1771	190 (0)	0.0510	± 15
2263 → 911	1342	113 (0)	0.0240	± 15
911 → 0	911	135 (0)	0.0180	± 20
E_x → 3453	1790			
3453 → 0	3440			
3128 → 2319	* 807	634 (0)	0.0384	± 13
	*1563	94 (0)	0.0223	± 15
	*1729	150 (0)	0.0685	± 15

E_p = 1.844 Mev figure 9.2g'

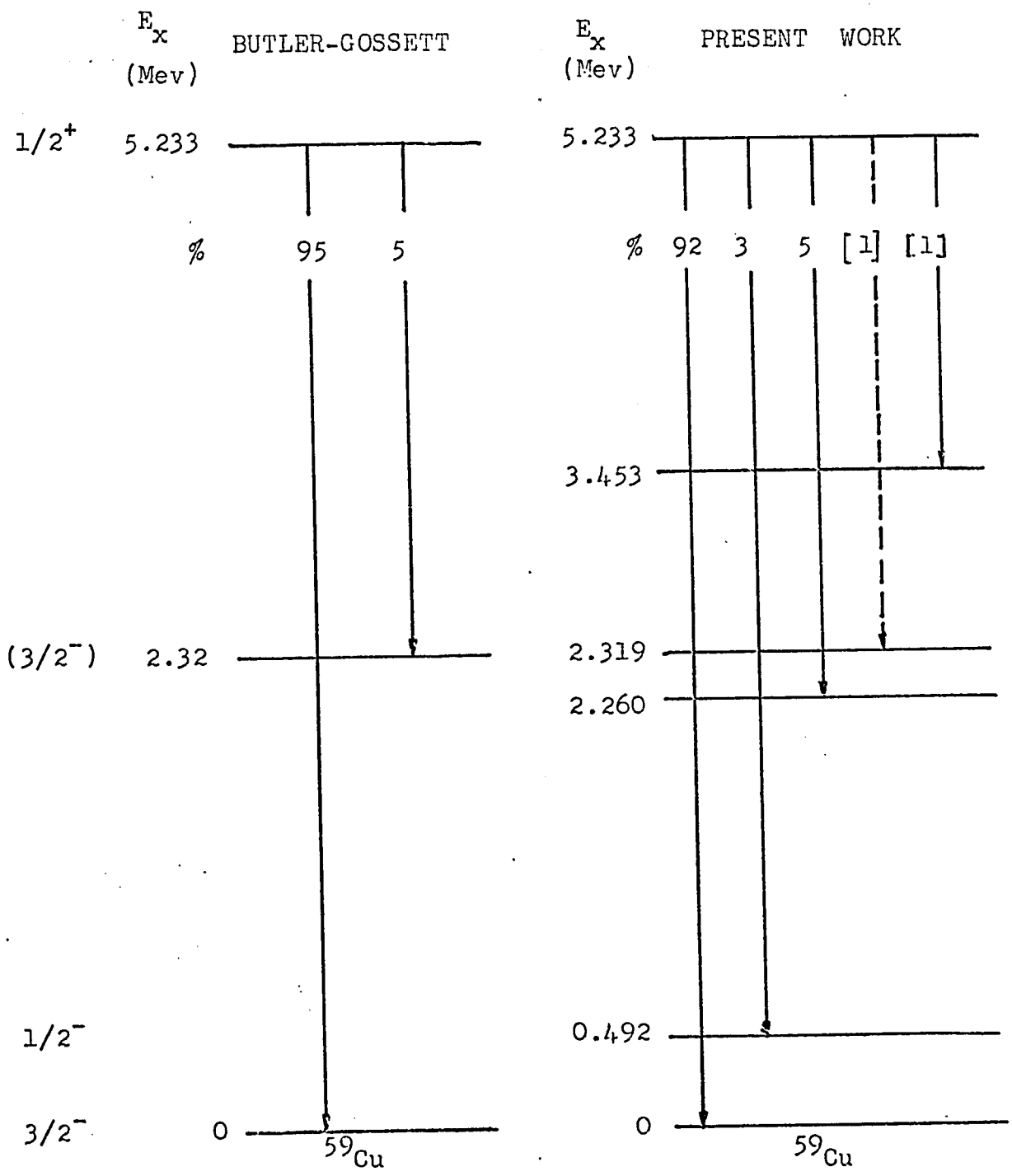

BRANCHING RATIOS OF RESONANCE LEVEL

and in table 8.2g respectively. The decay of the resonance level is characterized by a strong decay to ground. The transition to the 2319 kev level previously reported by Butler and Gossett is not observed and is less than 1% of the total decay. Three additional transitions are observed; two weak gamma rays to levels at 494 and 2260 kev and a weak transition to the 3453 kev level. The strength of the line to the 3453 kev level is less than 1% of the total decay. However the 90° spectrum clearly shows that the transition occurs. Three unexplained gamma rays were observed at 807, 1563 and 1729 kev. The energy of one of these is consistent with known energy differences between established levels in ^{59}Cu below 3128 kev.

8.2h THE 1883 KEV RESONANCE (E_x = 5.269 Mev)

The spectrum at 125° is shown in figure 8.2h. The analyzed data obtained from the spectra for the 1883 kev resonance is listed in table 8.2h and a resulting decay scheme for the resonance level is shown in figure 8.2k. As in the case of the 947 kev resonance a level at 1837 kev level reported previously only by Marusak and Stelson via the ^{58}Ni (d,n) ^{59}Cu reaction (Ma.,St.,67). The intensity of the 1291 kev gamma ray resulting from the 3128 → 1837 transition

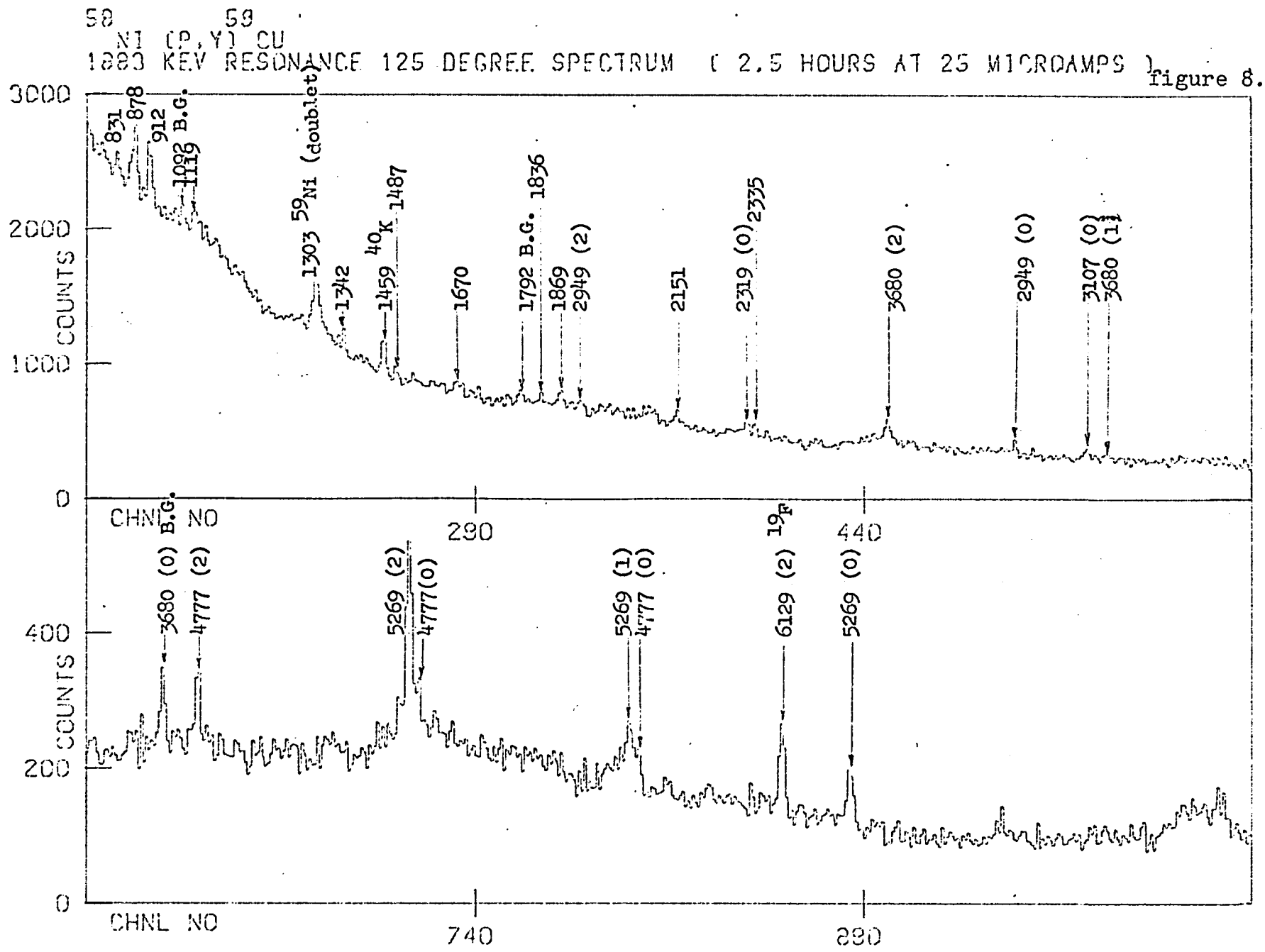
58 59
NI (P,Y) CU
1883 KEV RESONANCE 125 DEGREE SPECTRUM (2.5 HOURS AT 25 MICROAMPS)
3000
2000
1000
0
COUNTS
831
878
912
1098 B.G.
1119
1303 59Ni (doublet)
1342
40K 1459
1487
1670
1792 B.G.
1836
1869
2949 (2)
2151
2319 (0)
2335
3680 (2)
2949 (0)
3107 (0)
3680 (1)
CHNL NO
290
440
B.G.
19F
400
200
0
COUNTS
3680 (0)
4777 (2)
5269 (2)
4777(0)
5269 (1)
4777 (0)
6129 (2)
5269 (0)
CHNL NO
740
290

figure 8.2h

E_p = 1883 kev , E_x = 5270 kev

table 8.2h

TRANSITION	E_γ(kev) ± 4 kev	INTEGRATED COUNTS	I (intensity) $\times 10^{-6}$	ΔI %
E_x → 0	5269	226 (0)	2.67	± 13
E_x → 491	4777	249 (2)	0.955	± 17
491 → 0	491	--	--	
E_x → 2319	2949	100 (0)	0.545	± 15
2319 → 0	2319	141 (0)	0.530	± 15
E_x → 3128	2151	159 (0)	0.800	± 8
3128 → 1837	1291	577 (0)	1.12	± 35
1837 → 0	1836	110 (0)	0.250	± 8
1837 → 491	1342	210 (0)	0.420	± 25
911 → 0	* 912	(0)		
	*1119	240 (0)	0.401	± 30
	*1487	210 (0)	0.456	± 10
	*3107	188 (0)	1.12	± 15
	*1670	140 (0)	0.350	± 30
	*1869	245 (0)	0.689	± 10
	*2335	176 (0)	0.663	± 13

in ^{59}Cu was obtained by subtraction of the contribution due to a similar transition in ^{59}Ni which was calculated from the intensity observed for the 878 kev peak in ^{59}Ni. Several non-background gamma rays remain unexplained one of which corresponds to energy level differences in the known lower levels of ^{59}Cu. The decay of the 5269 kev resonance level is predominantly to ground and to the first excited state, this suggest a spin of 3/2 or 5/2 for the resonance level.

8.2i THE 1923 KEV RESONANCE (E_x = 5.297 Mev)

The spectrum at 125° for the 1923 kev resonance is shown in figure 8.2i. The tabulated data and a resulting decay scheme for the 5.297 Mev level are given in table 8.2i and figure 8.2k respectively. The decay is predominantly to the second excited state with spin and parity $5/2^-$, but de-excitation gamma rays show that the 1837 kev, the 2913 kev and the 491 kev levels are also populated, although the primary transitions are unobserved. The decay suggest a 3/2 or 5/2 spin for the resonance level. As for the 1837 kev level, the 1965 kev level populated by this resonance has been observed previously only by the ^{58}Ni (d,n) ^{59}Cu reaction. The 90° spectra shows

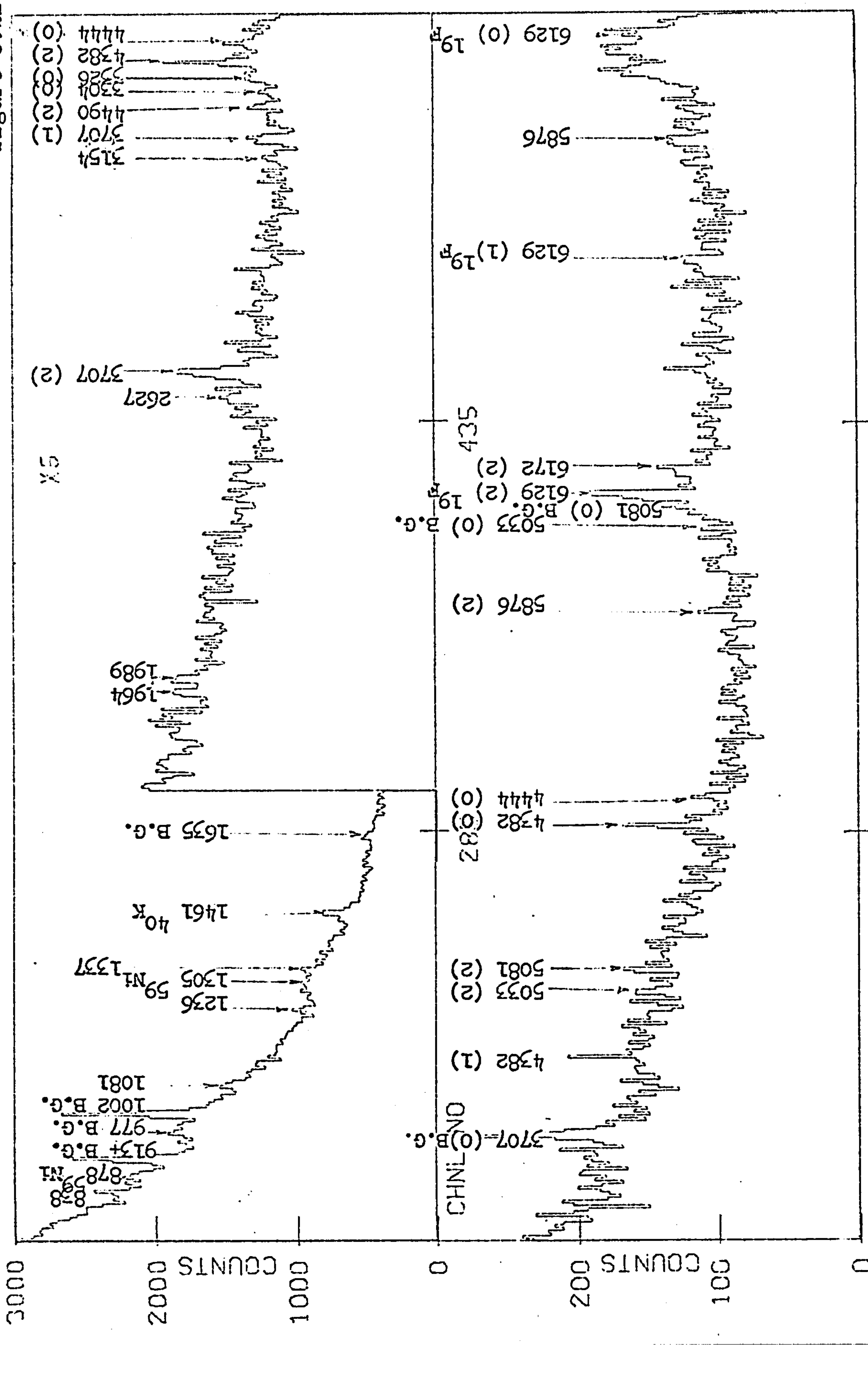

58NI (P,Y) 59CU
1923 KEV RESONANCE 125 DEGREE SPECTRUM (2 HOURS AT 25 MICROAMPS) figure 8.21

E_p = 1923 kev , E_x = 5297 kev

table 8.2i

TRANSITION	E_γ(kev) ± 4 kev	INTEGRATED COUNTS	I (intensity) x10^{-6}	ΔI %
E_x → 911	4382	110 (0)	1.00	± 15
911 → 0	913	1012 (0)	1.32	± 8
E_x → 1989	3304	43 (0)	0.268	± 25
1989 → 0	1989	100 (0)	0.284	± 15
E_x → 1962	3326	45 (0)	0.288	± 30
1962 → 0	1965	95 (0)	0.281	± 15
491 → 0	* 491	--	--	
	* 959	144 (0)	0.200	± 15
2913 → 1836	*1081	310 (0)	0.516	± 20
	*1236	250 (0)	0.454	± 15
	*1337	150 (0)	0.300	± 15
	*2627	60 (0)	0.279	± 16

a weak primary gamma ray feeding the 3709 kev level in ^{59}Cu. The cascade gamma ray to ground would be masked by the 3707 background gamma ray.

8.2j DECAY OF LOWER LEVELS

Information on the de-excitation of four of the lower excited levels was obtained. Results are shown in figure 8.2j. Previous worker have established the spins and parities of the 2319 and 3128 kev levels to be $1/2^-$ or $3/2^-$. If they are both $1/2^-$ rather than $3/2^-$, then the relatively strong transitions from the levels to the $5/2^-$ second excited state most probably would be electric quadrupole in character which would be consistent with the levels being due to collective excitation.

8.2k SUMMARY

All of the resonance levels studied were observed to decay directly to both the ground state and the first excited state with the exception of that at E_p = 1833 kev and E_p = 1923 kev. Three of the resonances (E_p = 1376, 1424 and 1716 kev) decay also to both the second excited state and the 1988 kev level. The 1833 kev resonance level which has its strongest branch to a possibly new level the 1398 kev level.

figure 8.2j

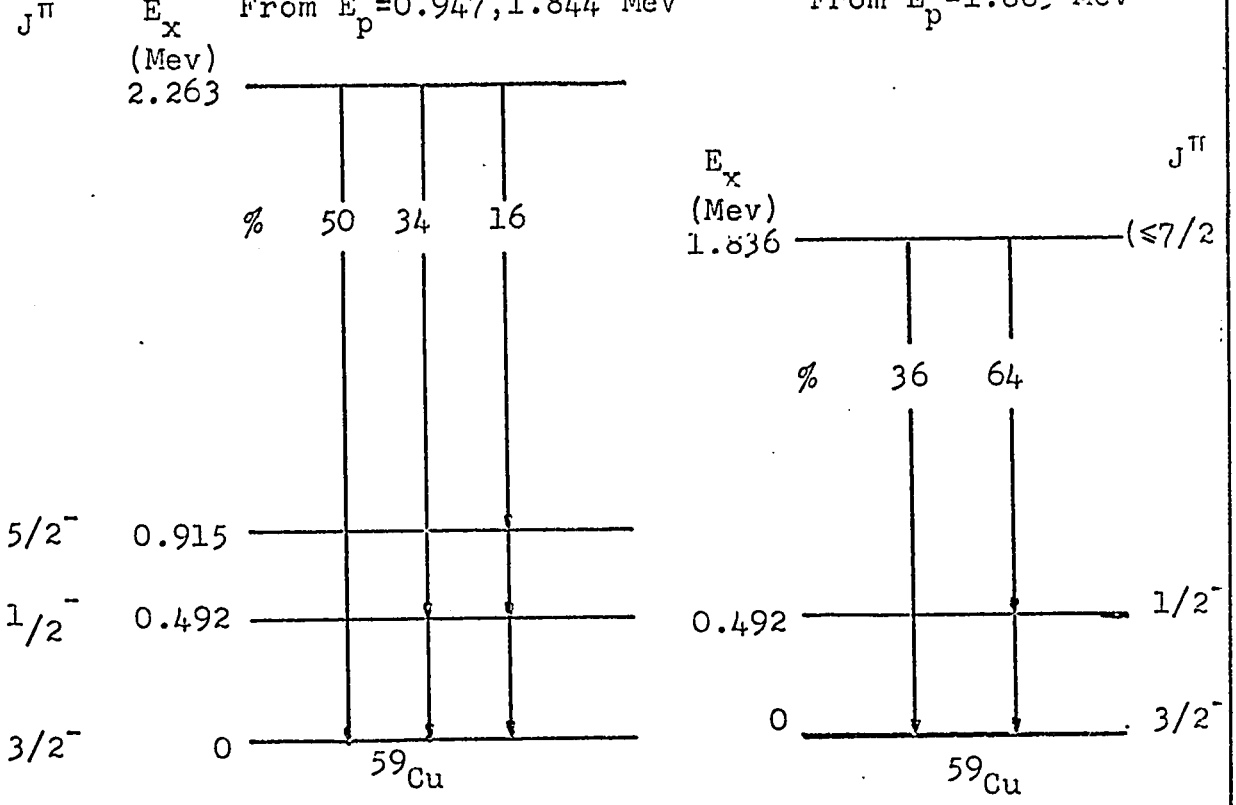

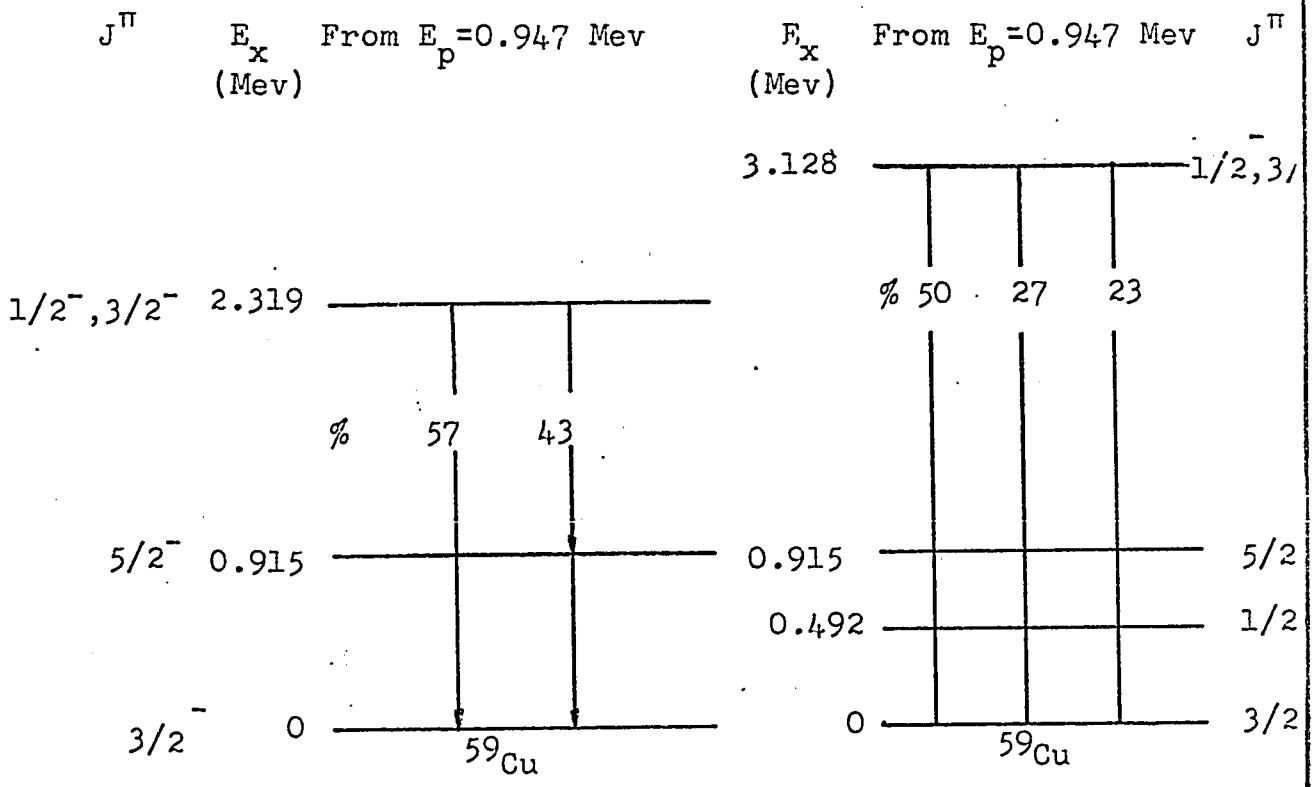

BRANCHING RATIOS OF LOWER LEVELS

figure 8.2k

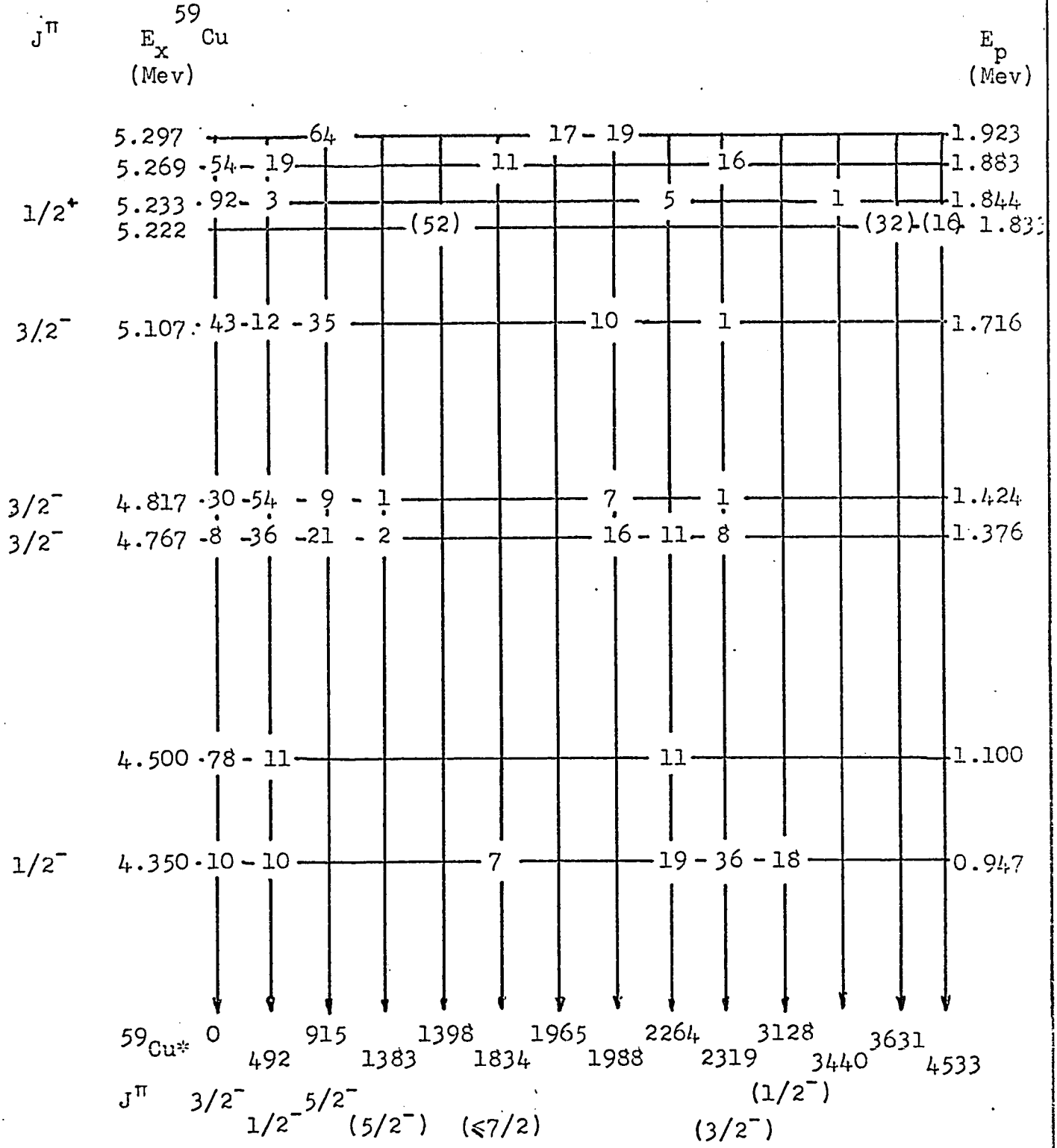

GAMMA DECAY OF ^{58}Ni (p,γ) ^{59}Cu RESONANCE LEVEL

The decay of the 947 kev and 1883 kev resonances confirm the existence of a level at 1837 kev excitation of energy. This level being previously observed only in the (d,n) stripping reactions. The 1923 kev resonance level populates a level at 1965 kev which has been observed previously only in (d,n) reactions also.

In table 8.2k are given the level positions in ^{59}Cu as established by the present radiative proton capture work. A star indicates that the level is not fully established but that there is evidence that the level is populated. Are also given the corresponding energy levels as observed in (d,n) and (^{3}He,d) stripping reactions.

8.3 BACKGROUND GAMMA RAYS

Listed in table 8.3 are the main background gamma rays which result from proton induced reactions for the resonant proton energies of ^{58}Ni studied. Not listed are those background gamma rays which can be classified as room background such as the 1461 kev gamma ray resulting from the positron decay of ^{40}K to the first excited state of ^{40}A and the 2615 kev gamma ray of thorium. As can be observed from

table 8.2k

Reference (Ma.,St.,67) E_γ(kev)	Reference (Pu.,Ro.,Ho.,67) E_γ(kev)	Present Work E_γ(kev)
479	497	491.8 ± 1
895	921	914.5 ± 1
1375	1401	1383 ± 1
		1398 ± 4
1837		1837 ± 3
1962		1965 ± 4
		1988 ± 4
2299	2275	2263 ± 3
2369	2325	2319 ± 3
2913		*2913 ± 4
3023	3046	*3040 ± 4
3114	3134	3128 ± 3
3427	3453	3453 ± 4
3654	3627	3627 ± 4
4358	4353	4353 ± 3
		4497 ± 3
	4550	*4550 ± 4
	4777	4767 ± 4
	4846	4817.6 ± 1
		5107 ± 4
		5222 ± 4
	5248	5233 ± 4
		5270 ± 4
		5297 ± 4

Backgroud γ- rays

table 8.3

E_p(kev)	Reaction	E_γ(Mev)	E_γ(Mev)$_{obs.}$ ± 4 kev
947	^{23}Na (p,p') ^{23}Na	0.444	0.441
	^{19}F (p,p')^{19}F	1.35	1.347
			2.164
			4.415
	^{15}N (p,αγ) ^{12}C	4.43	4.426
			4.452
			4.460
			4.956
	^{19}F (p,αγ) ^{16}O	6.129	6.129
1100			0.991
			1.290
	^{23}Na (p,γ) ^{24}Mg	1.366	1.369
			1.716
			2.160
			4.244
	^{15}N (p,αγ)^{12}C	4.43	4.418
			4.431
			4.452
			4.460
	^{19}F (p,αγ) ^{16}O	6.129	6.129

Background γ-rays

table 8.3(continued)

E_p(kev)	Reaction	E_γ(Mev)	E_γ(Mev)$_{obs.}$ ± 4 kev
1376	^{65}Cu (p,γ) ^{66}Zn	0.83	0.842
			0.945
			0.969
	^{14}N (p,γ) ^{15}O	1.39	1.400
			1.537
			3.209
			3.586
			4.221
			4.470
			4.512
			4.632
			4.797
	^{19}F (p,αγ)^{16}O		6.129
1424			0.810
	^{65}Cu (p,γ) ^{66}Zn	0.83	0.835
			0.990
	^{65}Cu (p,γ)^{66}Zn	1.040	1.040
			1.315
	^{23}Na (p,γ) ^{24}Mg	1.366	1.367
	^{14}N (p,γ) ^{15}O	1.39	1.411
	^{23}Na (p,αγ) ^{20}Ne	1.629	1.635
	^{19}F (p,αγ) ^{16}O	6.129	6.129

Background γ- rays

table 8.3(continued)

E_p(kev)	Reaction	E_γ(Mev)	E_γ(Mev)$_{obs.}$ ± 4 kev
1716			0.740
			0.788
			1.370
	$^{23}Na\ (p,\alpha\gamma)\ ^{20}Ne$	1.629	1.634
	$^{13}C\ (p,\gamma)\ ^{14}N$	3.53	3.525
			4.290
			4.928
	$^{19}F\ (p,\alpha\gamma)^{16}O$	6.129	6.129
1833			0.722
			0.996
	$^{65}Cu\ (p,\gamma)\ ^{66}Zn$	1.040	1.044
	$^{14}N\ (p,\gamma)\ ^{15}O$	1.39	1.400
	$^{23}Na\ (p,\alpha\gamma)\ ^{20}Ne$	1.629	1.632
			5.066
	$^{19}F\ (p,\alpha\gamma)^{16}O$	6.129	6.129
1844	$^{23}Na\ (p,\alpha\gamma)\ ^{20}Ne$	1.629	1.632
	$^{19}F\ (p,\alpha\ )^{16}O$	6.129	6.129
1883			0.996
	$^{65}Cu\ (p,\gamma)\ ^{66}Zn$	1.040	1.044
			1.092
			1.792
			3.680
			5.294
	$^{19}F\ (p,\alpha\gamma)\ ^{16}O$	6.129	6.129

Background γ-rays

table 8.3(continued)

E_p (Mev)	Reaction	E_γ (Mev)	E_γ (Mev)$_{obs.}$ ± 4 kev
1923	^{65}Cu (p,γ) ^{66}Zn	0.83	0.838
			0.977
			0.992
			1.002
	^{23}Na (p,αγ)^{20}Ne	1.629	1.635
			3.707
	^{15}N (p,αγ) ^{12}C	4.43	4.444
			5.033
			5.081
			5.460
	^{19}F (p,αγ) ^{16}O	6.129	6.129
			7.194

table 8.3 and the spectra most of the main background gamma rays are due to well known contaminants: $^{12,13}C$, $^{14,15}N$ and ^{19}F, these are the main sources of background gamma rays in proton induced reactions. Also observed are gamma rays whose energies correspond to transitions following proton induced reactions on $^{63,65}Cu$ and $^{64,66}Zn$. These would result if the proton beam is not adequately focussed and aligned along the axis of the target chamber and partially scrapes the brass walls of the chamber. These background gamma rays could be reduced by better monitoring of where the beam goes and what it looks like at different places along the beam line; in particular near the target chamber. Monitoring could be done electrically or (and) by using quartz-viewers. Plating with gold on the inside of the chamber would eliminate small shadow or reflection effects. As for background gamma rays originating from contaminants the problem is more serious. The ^{19}F contamination was observed to be due to a continuous build up of fluorine on the target and target chamber. It was found that a thorough water cleaning reduced the fluorine background by a factor of 10. The source of the fluorine contamination is attributed to the leaking of the insulating gas

SF_6 of the accelerator pressure vessel into the system. The potassium cyanide, KCN, used in the gold plating solution for electroplating gold on the target backings is a source of gamma rays due to reactions in nitrogen and carbon. No carbon build up was noticed.

8.4 CALCULATION OF THE Q OF $^{58}Ni\ (p,\gamma)\ ^{59}Cu$ REACTION

The Q value for radiative proton capture in the laboratory coordinate system can be written as:

$$Q = E_{\gamma 0} + E_{rp} + E_{r\gamma 0} - E_p \qquad (17)$$

where $E_{\gamma 0}$ is the energy of the ground state gamma ray or the sum of any cascade leading to ground, E_{rp} is the recoil energy of the residual nucleus due to proton capture, $E_{r\gamma 0}$ is the recoil energy due to gamma ray emission and E_p is the energy of the incident proton.

Accurate energy measurement of the so-called 1424 and 1844 kev resonances was made by Bondelid and Kennedy (Bo.,Ke.,59) using electrostatic analyser and deflection at 90^o. They determine the energies to be 1424.1 ± 0.7 kev and 1843.7 ± 0.9 kev respectively. The unshifted energy of the ground state gamma ray

for both resonances was measured with the Ge(Li) spectrometer and found to be 4817.4 ± 1 kev and 5233 ± 3 kev for the 1424 and 1844 kev resonances respectively. E_p and $E_{\gamma 0}$ being well determined the two other terms of equation (17) were calculated. For calculating E_{rp} term the mass of the ^{59}Cu isotope was obtained from the atomic mass table of J.H.E. Mattauch (Ma.,Th.,Wa.,65). The best calculated value is Q = 3417.5 ± 1.7 kev the weighted average value is Q = 3418.5 ± 2.4 kev. Both values are in agreement within experimental uncertainties with the value obtained by Butler and Gossett which is 3.42 ± 0.02 Mev.

8.5 DOPPLER SHIFT

One of the techniques used to determine nuclear lifetimes is the Doppler shift attenuation method. If a gamma ray is emitted by a moving nucleus its detected energy will be dependent on the velocity of the nucleus. If this velocity can be changed continuously in a known way between the formation of the excited nucleus and the decay, one can in principle measure a lifetime.

The usual way is to slow down a nucleus, formed by a particle reaction, by letting it recoil in the target material and/or backing. If the lifetime is

longer than the time it takes the nucleus to come to rest, the gamma ray energy is independent of direction. This will give a lower limit on the lifetime. Likewise if the decay is very fast the full shift will be seen since the nucleus will not have had time to slow down. This will give an upper limit. For the case when the gamma ray is emitted with the nucleus in motion one will observed an attenuated Doppler shift, from which one can, in principle deduce a value of the lifetime.

If the excited nucleus is formed by radiative capture, the energy of the emitted gamma ray at an angle θ with respect to the direction of the beam (i.e. the direction of recoil) is given by:

$$E(\theta) = E_0(1 + \frac{v}{c} \cos\theta) \qquad (18)$$

where E_0: unshifted gamma ray energy

v: velocity of recoiling nucleus

c: velocity of light.

If the velocity of the recoiling nucleus is decreased between capture of the incident particle and the decay, the Doppler shift will be attenuated.

The fractional change in the gamma ray energy is:

$$\frac{\Delta E(t)}{E_0} = \frac{E(\theta) - E_0}{E_0} = \frac{v(t)}{c} \cos\theta \tag{19}$$

where v(t) is the velocity at a time t. The number of nuclei that decay at anytime t, per initial nucleus, is:

$$n(t) = e^{-t/\tau} \tag{20}$$

where τ is the mean life. Therefore the change of the number of excited nuclei in a time interval dt following t is:

$$d\, n(t) = - \frac{e^{-t/\tau}}{\tau} dt \tag{21}$$

and the number of gamma rays emitted is:

$$- d\, n(t) = \frac{e^{-t/\tau}}{\tau} dt \tag{22}$$

This means that the average fractional change is:

$$\frac{\Delta E}{E_0} = \int_0^\infty \frac{e^{-t/\tau}}{\tau} \frac{v(t)}{c} \cos\theta \, dt \qquad (23)$$

so that the average energy of a gamma ray emitted at an angle θ is:

$$\bar{E}(\theta) = E_0 \left[1 + \left(\frac{1}{v_0 \tau} \int_0^\infty e^{-t/\tau} \, v(t) \, dt\right) \frac{v_0}{c} \cos\theta\right] \qquad (24)$$

or:

$$\bar{E}(\theta) = E_0 \left(1 + F(\tau) \frac{v_0}{c} \cos\theta\right) \qquad (25)$$

where:

$$F(\tau) = \frac{1}{v_0 \tau} \int_0^\infty e^{-t/\tau} \, v(t) \, dt \qquad (26)$$

and v_0 is the value of v(t) at t = 0. v(t) depends on the material in which the recoiling nucleus is slowing down, on the initial velocity and on the recoiling nucleus itself. The change in velocity is related to the energy loss as follows:

$$M \frac{dv}{dt} = \frac{dE}{dx} \tag{27}$$

here M is the mass of the recoiling nucleus. A sufficient approximation is to take the energy loss of the moving particle to be proportional to the velocity that is:

$$- \frac{dE}{dx} = - \frac{M}{\alpha} v \tag{28}$$

the above equation gives:

$$v(t) = v_0 \, e^{- t/\alpha} \tag{29}$$

is called the characteristic slowing down time. This is usually of the order of 10^{-13} second. Experimentally

it is found that α differs little for different ions slowing down in the same material. However, α depends upon the material in which the ions slow down.

Substitution of the expression for $v(t)$ into $F(\tau)$ gives:

$$F(\tau) = \frac{\alpha}{\alpha + \tau} \qquad (30)$$

If τ is approximately $\alpha/10$ then $F(\tau)$ is approximately 0.9 which is difficult to observe experimentally. This is the reason why attenuated Doppler shift measurements are useful only for determinating half lives roughly between 10^{-11} and 10^{-14} second. For lifetimes outside this range it is usually possible only to place limits on the lifetime. Ge(Li) detectors, because of their higher resolution, make it possible to detect much smaller shifts than was possible with NaI (Tl) detectors. This means that smaller recoil velocities can be used and a greater range of lifetimes measured. In order to deduce the lifetime from an observed value of $F(\tau)$ a knowledge of the slowing down mechanism of particles moving through matter is important. The mechanism by which slow

moving ions can lose energy is:

1) by collisions with electrons
2) by collisions with atoms

The collisions with the atom not only cause a loss in energy but also a change in direction of the recoiling nucleus which will influence the detected Doppler-Shift. Blaugrund (Bl.,66) has shown that the change in direction is usually more important than the energy loss due to atomic collisions therefore $F(\tau)$ is now:

$$F(\tau) = \frac{1}{v_0 \tau} \int_0^\infty v(t) \langle \cos\Phi \rangle \, e^{-t/\tau} \, dt \qquad (31)$$

in which $\langle \cos\Phi \rangle$ is the average value of $\cos\Phi$ at a time t. Φ is the angle with the initial recoil direction. Recalling that average value of gamma ray emitted at an agle θ is:

$$\bar{E}(\theta) = \bar{E}(90^\circ) \left[1 + F(\tau) \frac{v_0}{c} \cos\theta\right] \qquad (32)$$

The observed shift between two measurements performed at 0° and 90° is:

$$\bar{E}(0^\circ) - \bar{E}(90^\circ) = \bar{E}(90^\circ)\, F(\tau)\, \frac{v_0}{c} \qquad (33)$$

so that an experimental value for $F(\tau)$ can be determined by measuring $\bar{E}(90^\circ)$ and $\bar{E}(0^\circ) - \bar{E}(90^\circ)$ which would give:

$$F(\tau) = \frac{\bar{E}(0^\circ) - \bar{E}(90^\circ)}{\Delta E} \qquad (34)$$

where $\Delta E = \bar{E}(90^\circ)\, \frac{v_0}{c}$ and is the full shift which can be calculated, or measurement at several values of θ allows $F(\tau)$ to be deduced from a plot of E_γ against $\cos\theta$. In the case of proton capture on a nucleus of atomic mass number, A, the initial recoil velocity v_0 can be calculated from:

$$\tfrac{1}{2} M v_0^2 = E_p/A + 1 \qquad (35)$$

where E_p is the incident proton energy and M is the mass of the compound excited nucleus.

Doppler shift data was obtained for the E_p = 1424 kev resonance level from the analysis of the spectra accumulated while attempting the angular distribution previously mentioned in section 4.4. Using a thick target (approximately 20 kev), the ground state gamma ray showed an observable shift, for measurements performed at 0° and 90°, of about 4 kev. Which is approximately the full shift value. The data was corrected for electronic drifts by using the 511 kev anihilation peak and the second escape peak due to fluorine as internal energy calibration points. The resulting data is shown in figure 8.5a and shows clearly the observed shift. A full line corresponds to the position of the first escape peak plus 511 kev. The data was not corrected for changes in the non-linearity due to electronic drifts since a drift of 10 channels would at maximum produce a change .05 channels in the non-linearity. The value of the observed gamma ray energy $\overline{E}(\theta)$ at each angle was obtained by doing a weighed average of the full energy peak and its escape peaks. The weighting factor being the square root of the number of integrated counts of each peak. Plots of $\overline{E}(\theta)$ as a function of $\cos\theta$ were

Figure 8.5a

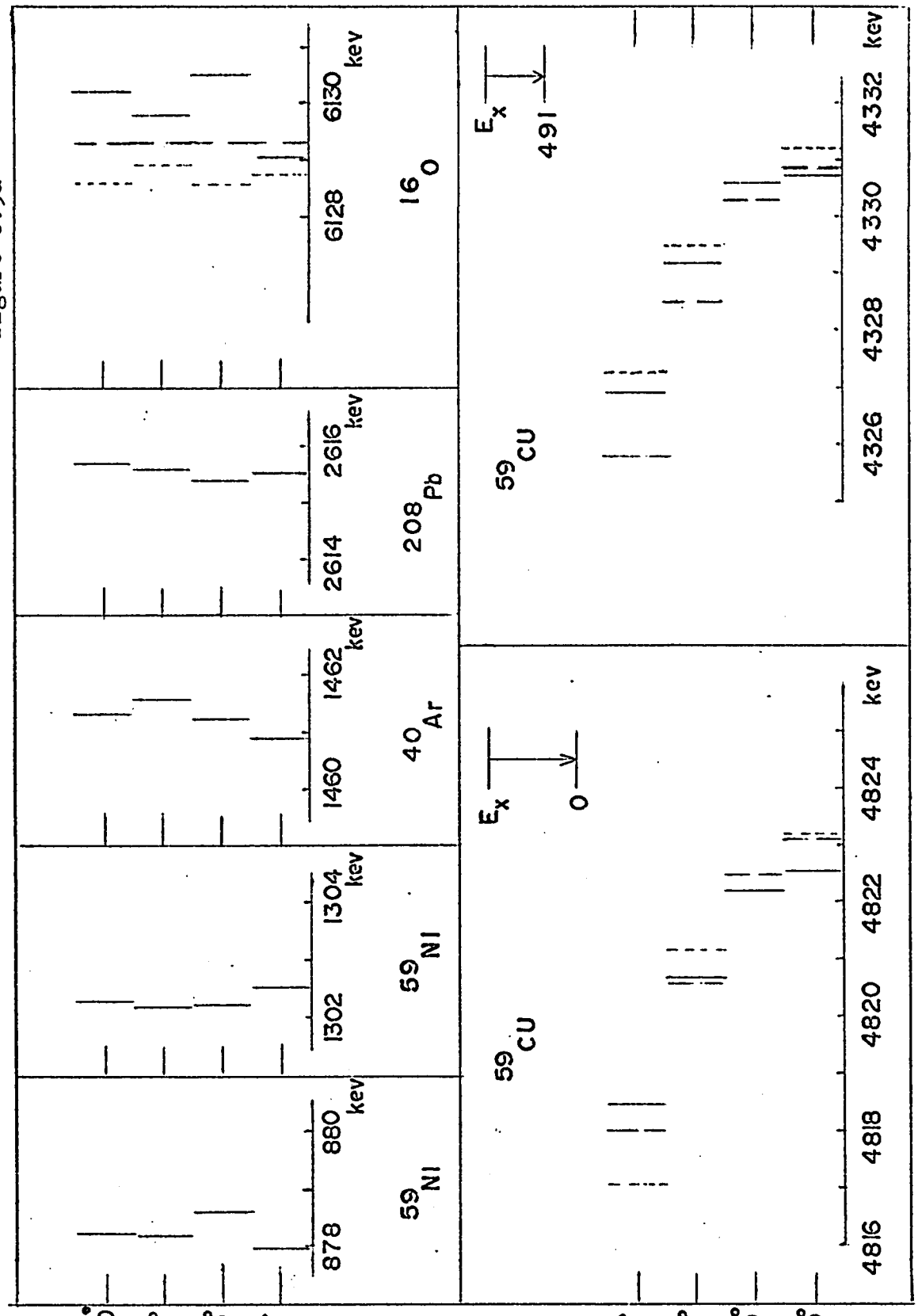
90°
60°
30°
0°
878
880 kev
59 Ni
1302
1304 kev
59 Ni
1460
1462 kev
40 Ar
2614
2616 kev
208 Pb
6128
6130 kev
16 O
E_x
0
59 Cu
4816
4818
4820
4822
4824 kev
E_x
491
59 Cu
4326
4328
4330
4332 kev

done and are shown in figure 8.5b and figure 8.5c for the ground state gamma ray and for the gamma ray going to the first excited level respectively. The values of $F(\tau)$ so obtained are $F(\tau) = 1.05 \pm {}^{.07}_{.08}$ for the ground state transition and $F(\tau) = 1.02 \pm {}^{.09}_{.08}$ for the transition to the first excited level. Calculations of $F(\tau)$ as a function of τ were done using a program developped by A. Lachaîne which uses the Blaugrund formulation for calculating $F(\tau)$. The resulting curve is shown in figure 8.5d and gives $\tau < 2 \times 10^{-15}$ second. The total partial gamma ray width, Γ_γ, calculated for this resonance in section 8.1 gives $\tau \geq 1.3 \times 10^{-15}$ second. The uncertainty in τ is $\pm$ 15% for the Doppler shift result and the uncertainty in τ from the partial gamma ray width calculation was estimated to be $\pm$ 25%.

9. DISCUSSION

9.1 THEORETICAL

The simplest core excitation model predicts a low lying quadruplet of states in ^{59}Cu with $J^\pi = 1/2^-$, $3/2^-$, $5/2^-$ and $7/2^-$, formed by coupling

figure 8.5b

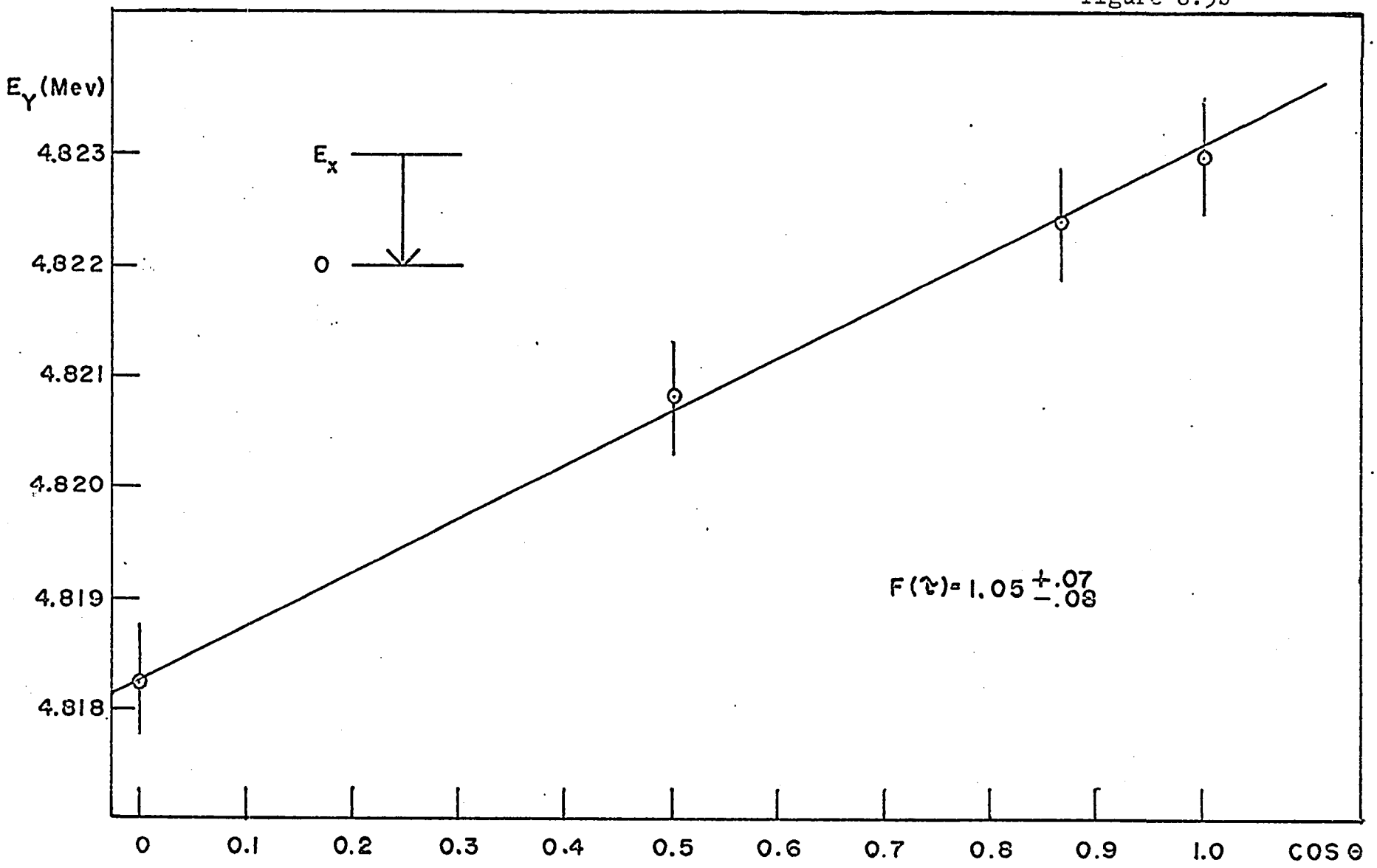
E_γ (Mev)
4.823
4.822
4.821
4.820
4.819
4.818
E_x
0
$F(\hat{\gamma}) = 1.05 \pm .07 \\ -.08$
0
0.1
0.2
0.3
0.4
0.5
0.6
0.7
0.8
0.9
1.0
COS Θ

figure 8.5c

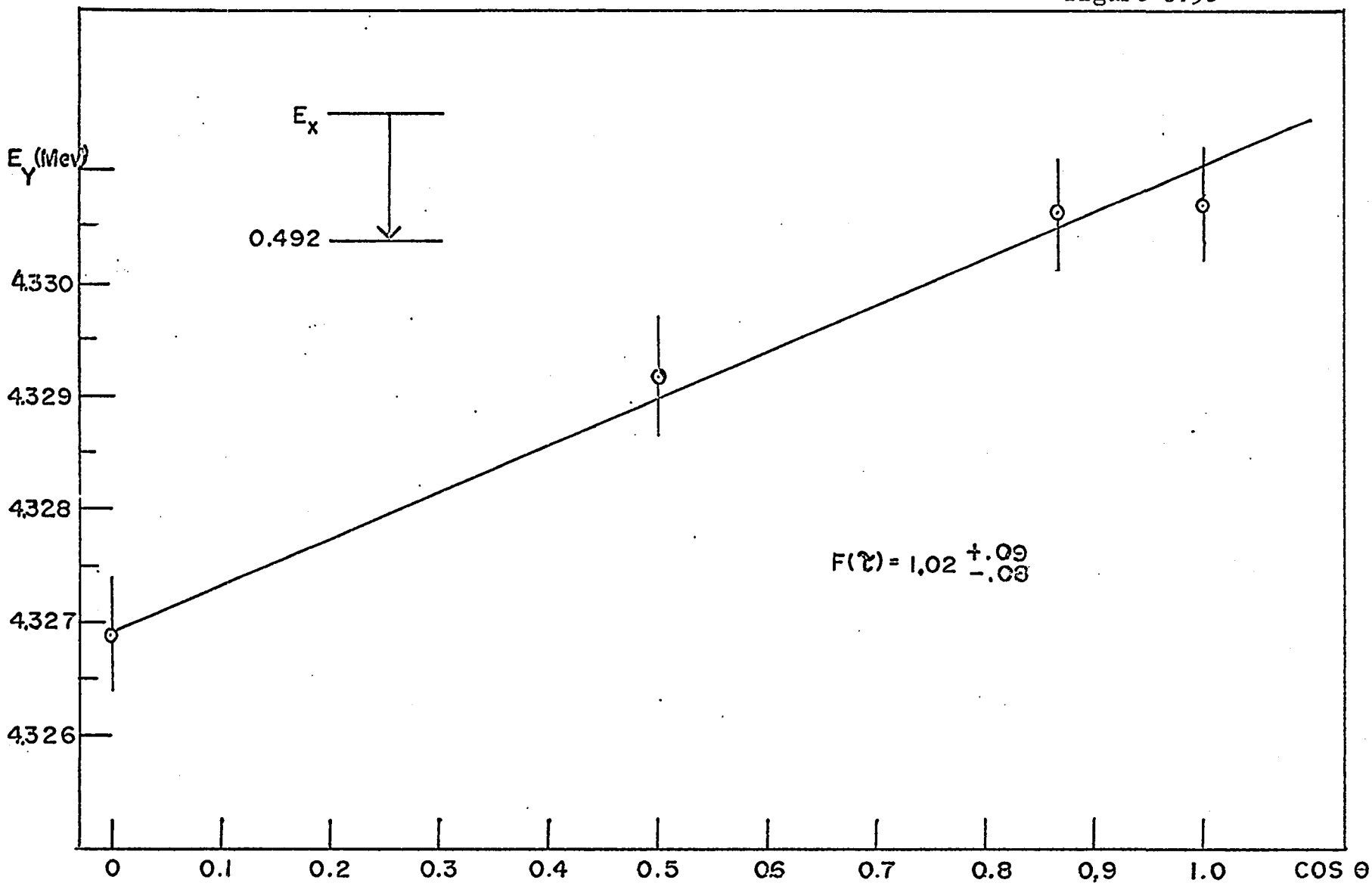
E_x
0.492
E_γ (Mev)
4.330
4.329
4.328
4.327
4.326
$F(\gamma) = 1.02 \pm .09 \pm .03$
0
0.1
0.2
0.3
0.4
0.5
0.6
0.7
0.8
0.9
1.0
COS θ

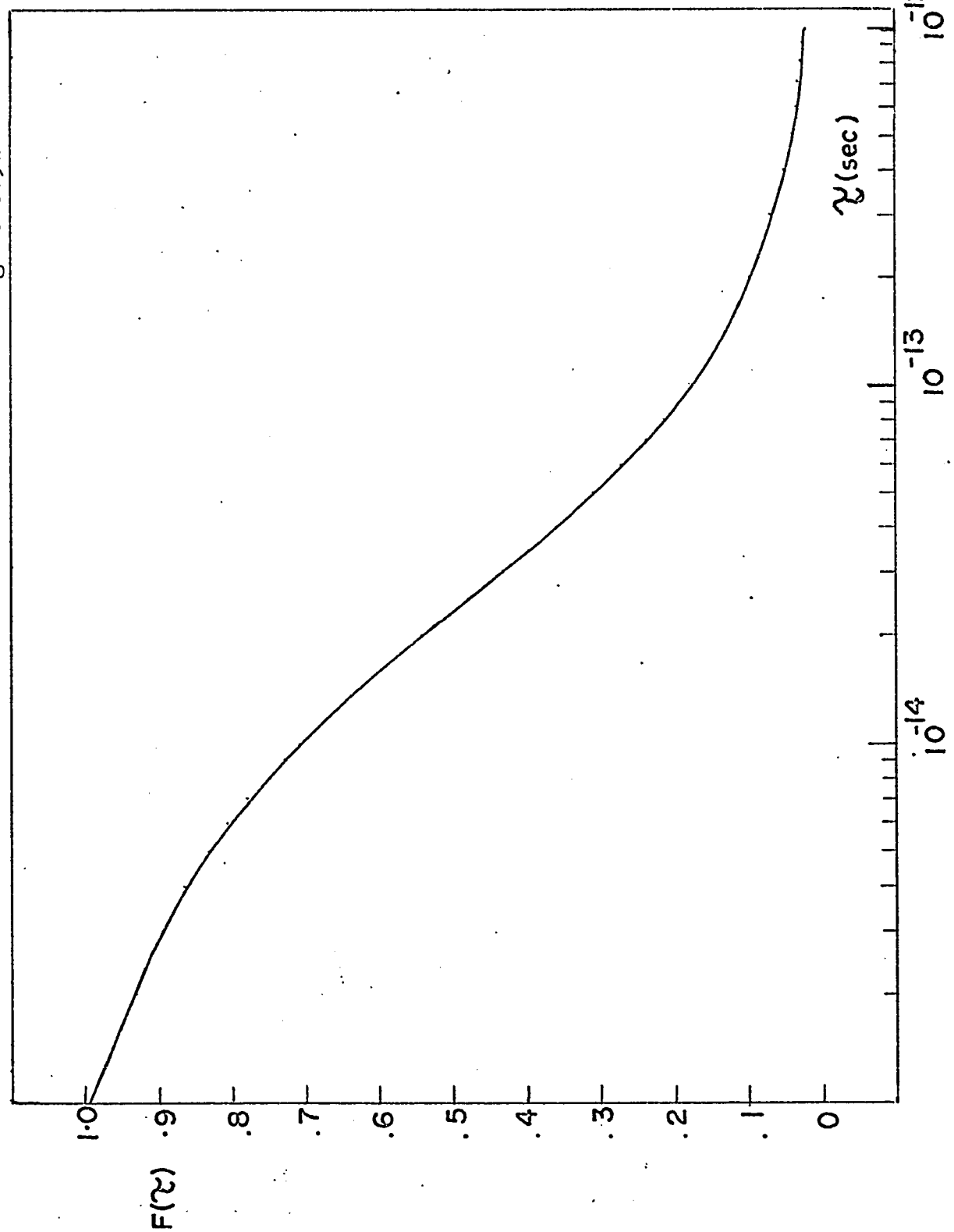

figure 8.5d

the odd $2p_{3/2}$ proton to the first excited one phonon 2^+ state of ^{58}Ni. However (^3He,d) stripping reactions show spectroscopic strengths for most of the low lying states of ^{59}Cu which have large amounts of 2p and 1f single particle strengths (Bl.,64), (Mo.,Sc.,66), (Pu.,Ro.,Ho.,67).

These observations are more consistent with extended models, such as the unified model of Bouten and Van Leuven (Bo.,Va.,62) in which a $2p_{3/2}$, $2p_{1/2}$ and $1f_{5/2}$ proton is allowed to couple with the ground, one and two phonon states of the Ni-core.

The ^{58}Ni (^3He,d) ^{59}Cu work of Pullen and Rosner (Pu.,Ro.,Ho.,67) leads them to suggest that 1.40 Mev and the 2.27 Mev levels are the only two candidates for the expected $7/2^-$ state at around 1.3 Mev of excitation predicted by the calculations of Bouten and Van Leuven. From the present work the decay of the 947 kev resonance level corresponding to E_x = 4.351 Mev with $J^\pi = 1/2^-$ shows a 19% branch to the 2.263 Mev level; this rules out the 2.27 Mev level as being a candidate for the expected $7/2^-$ state since the favored type for this transition would be an M3 which is most unlikely. Blair (Bl.,64) has suggested that

more than one level may be excited at around 1.40 Mev. However this is not apparent from Pullen & Rosner's study since no state is observed in the deuteron spectrum with a separation greater than 15 kev from the known level at 1.401 Mev. The present $^{58}Ni\ (p,\gamma)\ ^{59}Cu$ work shows that two levels do actually exist in this region of excitation one at 1.383 Mev and one at 1.398 Mev. The 1.398 Mev level is populated strongly only by the 1833 kev resonance. This resonance is very weak and is observed to populate only three levels: (52)% to the 1.398 Mev level, (32)% to the 3.627 Mev level and (16)% to the 4.550 Mev level. All three levels are of unknown spins. As mentioned previously in section 8.2f, because it is very weak the 1833 kev resonance is probably a high spin state. This would indicate that the 1.398 Mev level is also a high spin state, possibly 7/2. Since the 1.383 Mev level was observed to be weakly populated only by the 1376 and 1424 kev resonance levels which both have a spin of $3/2^-$ the spin of this level is most probably 5/2. The level positions and the arguments pertaining to the spins of the 1.383 and 1.398 Mev levels are in agreement with the Bouten and Van Leuven unified

model as shown in figure 9.1.

The de-excitation of all the resonance levels studied are typical of single particle excitation with the exception of the 947 kev resonance level whose decay indicates collective effects. This resonance should have a fast M1 transition to ground but instead it decays predominently to the 2.263, 2.319 and the 3.128 Mev levels which are approximately at half the excitation energy of the resonance level which is E_x = 4.351 Mev. This suggests a 2 phonon collective state. An angular correlation on these cascading gamma rays would indicate if the above is true since they would have to show a large E2 component with some M1 mixing. So that the decay of this level suggests that the 4.351 Mev level is probably a proton coupled to a 2 phonon state of the vibrating Ni-core while the 2.263, 2.319 and 3.129 Mev levels consist in a proton coupled to a one phonon vibrational state.

The transition strengths relative to the Weisshopf estimate yield have an average value of $|M|^2$ = .04 which is in no way indicative of collective excitation. However out of the nine resonant compound

figure 9.1

Experimental and theoretical energy spectra

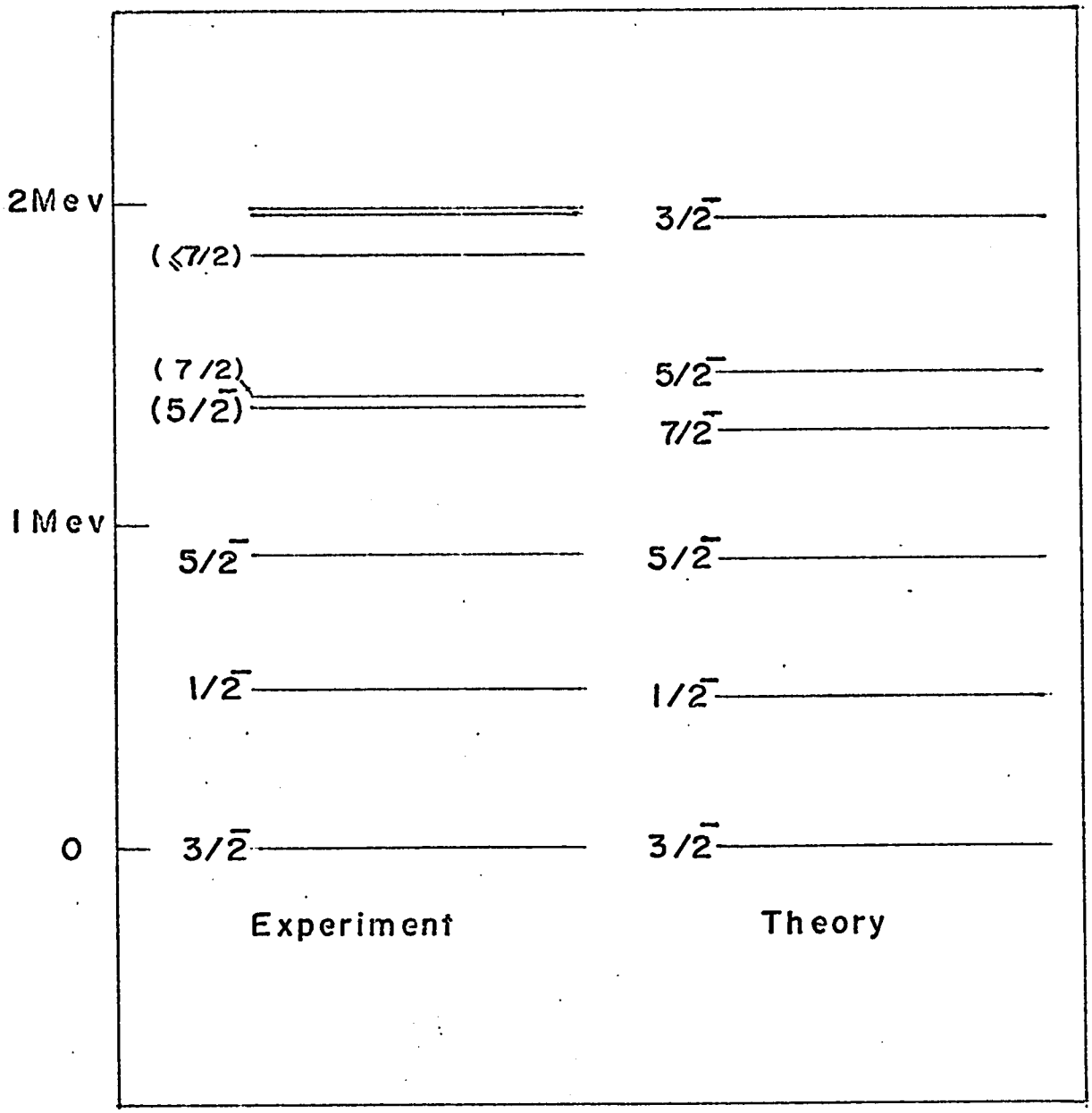

$^{59}_{CU}$

states formed, four have not been reported populated in ^{58}Ni (^{3}He,d) ^{59}Cu reaction these are the excited states corresponding to E_p = 1100, 1716, 1833 and 1923 kev. Hence showing some indication of collective excitation at these energies of excitation.

9.2 EXPERIMENTAL

The use of a high beam current accelerator to study reactions which have relatively low yields can only be exploited fully under low background conditions, since only then can full advantage be taken of the high beam current. The results obtained from the present study show that although much additional information was obtained for ^{59}Cu, a reduction of the proton induced background would have been very desirable and possibly would have yielded additional information.

The precise energy calibration now obtainable with spectrometer system no. 2 can be exploited usefully both in Doppler shift measurements and also in the determination of a decay scheme since consistency of energy sums for cascading gamma rays is more selective. The high resolution Ge(Li) detector reveals more clearly the level structure of nuclei

and gives more detail on the gamma ray decay of different levels. Although theory can in many cases barely explain more than the gross features of the nuclear structure, the additional detailed information obtainable with the Ge(Li) spectrometer is by no means superfluous since the main features so obtained are better established while the more detailed information obtained may lead to a deepened understanding of what processes are important in determining the nuclear structure and its properties.

REFERENCES

(Aa.,Cl.,Tr.,54) Aarset, B., Cloud, R.W., and Trump, J.G.
J. Appl. Phys., 25, 1365.

(Au.,69) Aubin, G., Barrette, J., Barette, M. and Monaro, S.
Nucl. Instr. and Meth., 76, 93-99.

(Bl.,64) Blair, A.G., Compt. Rend. Congrès International de Physique nucléaire, vol. 11, Paris, France, P. Gugenberger, ed. Centre National de la Recherche Scientifique (Paris), p. 471 (1964).

(Bl.,66) Blaugrund, A.E.
Nucl. Phys., 88, 501.

(Bo.,Bo.,68) Bouten, M.-C. and Bouten, M.
Physica, 40, 213-222.

(Bo.,Ke.,59) Bondelid and Kennedy.
Phys. Rev., 115, 1601.

(Bo.,Va.,62) Bouten, M. and Van Leuven, P.
Nucl. Phys., 32, 499-503.

(Bur.,49) Burtt, B.P.
Nucleonics, 5, 43, (August).

(Bu.,59) Butler, J.W.
Table of (p,γ) resonances, N.R.L. report 5282, U.S. Naval Research Laboratory, Washington D.C.

(Bu.,Go.,57) Butler, J.W. and Gossett, C.R.
Phys. Rev., 108, 1473-1495.

(Cr.,60) Crut, M. et al.
Nucl. Phys., 17, 655.

(En.,De.,59) Endt and Demeur
Nuclear reactions, vol. 1, p. 259.

(Ev.,53) Evans
The Atomic Nucleus, p. 904.

(Ka.,67) Kane, W.R. and Mariscotti, M.A.
Nucl. Instr. and Meth., 56, 189-196.

(Kr.,Ni.,Ba.,61) Kronenberg, S., Nilson, K., Basso, M.
Phys. Rev., 124, 1709.

(Ma.,68) Marion, J.B.
Nuclear Data, A4, 301-319.

(Ma.,St.,67) Marusak, A., Stelson, P.H.
private communication.

(Ma.,Th.,Wa.,67) Mattauch, J.H.E., Thiele, W., Waptra, A.H.
Nucl. Phys., 67, 1-31.

(Mo.,Sc.,66) Morrison, G.C., Schiffer, J.P.
Isobaric spin in nuclear physics, J.D. Fox and D. Robson, eds., Academic Press, p. 748.

(Pu.,Ro.,Ho.,67) Pullen, D.J., Rosner, B., Holbrow, C.H.
Phys. Rev., (to be published).

(Sl.,Ba.,56) Sliv, L.A., Band, I.M.
Coefficients of internal conversion of gamma radiation part 1, Academy of Sciences of the U.S.S.R., issued in U.S.A. as Report 57 ICCK1. Physic Department University of Illinois.

(Te.,He.,56) Temmer, G.M., Heydenberg, N.P.
Phys. Rev., 104, 967.

(Wi.,56) Wilkinson, D.H.
Phil. Mag., 1, 127.